frontiers | Frontiers in Earth Science

TYPE Original Research
PUBLISHED 12 September 2023
DOI 10.3389/feart.2023.1219351

OPEN ACCESS

EDITED BY
Laura Giambiagi,
CONICET Mendoza, Argentina

REVIEWED BY
Frederic Mouthereau,
Université Toulouse III Paul Sabatier, France
Cesar Witt,
Université de Lille, France

*CORRESPONDENCE
Lucas M. Fennell,
lucasfennell90@gmail.com

RECEIVED 09 May 2023
ACCEPTED 30 August 2023
PUBLISHED 12 September 2023

CITATION
Fennell LM, Martos FE, Peluffo NA, Acevedo E, Fernández Paz L, Morel L, Scazziota M, Naipauer M, Hauser N, Litvak VD and Folguera A (2023), The classical Cuevas River section revisited: an update to the style and timing of deformation of the Aconcagua region based on new geological, structural and geochronological data (32°50′S). *Front. Earth Sci.* 11:1219351. doi: 10.3389/feart.2023.1219351

The classical Cuevas River section revisited: an update to the style and timing of deformation of the Aconcagua region based on new geological, structural and geochronological data (32°50′S)

Lucas M. Fennell[1]*, Federico Exequiel Martos[2], Nicolás A. Peluffo[2], Eliana Acevedo[1], Lucía Fernández Paz[1], Luciano Morel[2], Mauro Scazziota[1], Maximiliano Naipauer[2], Natalia Hauser[3], Vanesa D. Litvak[1] and Andrés Folguera[1]

[1]CONICET, Instituto de Estudios Andinos Don Pablo Groeber (IDEAN), Universidad de Buenos Aires, Buenos Aires, Argentina, [2]CONICET, Instituto de Geocronología y Geología Isotópica (INGEIS), Universidad de Buenos Aires, Buenos Aires, Argentina, [3]Laboratory of Geochronology and Isotope Geochemistry, Instituto de Geocências, Universidade de Brasilia, Brasilia, Brazil

The Aconcagua region constitutes a classical site to study the growth of the Andes, being host of the highest mountain of South America and focus of numerous investigations since its first description by Charles Darwin almost 200 years ago. The last detailed works in this area characterized it as a typical thin-skinned fold-thrust belt with a basal detachment located in the lower evaporitic units of the Mesozoic sequences. Previous authors in this area correlated the different thrust sheets on the basis of their marine fossils, sedimentological characteristics and structural relations. Although these criteria were useful for the identification of the marine and evaporitic units, the resemblance between the nonmarine red beds and among the different volcanic units has difficulted their unequivocal assignment. Moreover, the inaccessibility of the outcrops and the lack of an adequate geochronological control has led to underestimate the importance of the Aconcagua fold-thrust belt in the last couple of years, being characterized as a secondary feature in Andean orogenesis. A series of new field observations, sedimentological studies and geochronological analyses were performed to update the geological map of this area and build a schematic cross section along the Río Cuevas at 32°50′S in west-central Argentina. These studies allowed the identification of important variations on the thickness of the Upper Jurassic nonmarine sequences associated with the activity of normal faults and the development of structural highs. Many of these normal faults are presently inverted, which suggests that tectonic inversion played an important role in the structuration of this region, leading to a deformational style that varies from a thick-skinned inner domain towards a thin-skinned frontal sector. A series of sedimentological profiles aided by four new U-Pb detrital zircon analyses and its integration with new geochronological databases allowed the documentation of previously unrecognized Paleogene deposits, the age reassignation of several volcanic and sedimentary units and the modification of the stratigraphy. Finally, at least three contractional events with different structural mechanisms were

identified along this transect, revealing a dynamic tectonic evolution that underscores the role of structural inheritance and the relevance of the Aconcagua fold-thrust belt in the Andean orogeny.

KEYWORDS

thin-skinned, thick-skinned, hybrid style, tectonic inversion, Late Jurassic extension

1 Introduction

The word Andes is derived from the Quechua word *Antis*, which makes reference to a tribe that lived in the high mountains east of Cuzco (Perú), once the capital of the Inca Empire. Since the name Andes was first coined by Inca Garcilazo de la Vega (1609), these mountains have been a magnet to a plethora of explorers, searching to describe them and unravel their origin. Nowadays, it is well-known that the Andes are the longest subduction-type orogen in the world, product of the convergence between the continental South American plate and a series of oceanic plates over several millions of years (e.g., Gansser, 1973; Ramos, 2009). As a consequence, the western margin of South America has been deformed generating a great diversity of orogenic systems grouped within the Andean Cordillera (Kley et al., 1999; Horton and Folguera, 2022). The Andes have an extension of more than 7,000 km of extension, but a particular sector is of great interest to scientists as it is home to the highest mountain in South America (Cerro Aconcagua, 6,960 m.a.s.l.): the Aconcagua region (Figure 1) (see Aguirre-Urreta and Ramos, 1996a for a review).

The Aconcagua region (32°30′-34°15S) is located in the Southern Central Andes, a sector of the Andean Cordillera comprised between 27° and 46°30S that can be subdivided, north and south of 33°30S, into two general segments: the flat slab subduction segment to the north and the normal subduction segment with a 30° dip to the south (Ramos, 1999; Giambiagi et al., 2022a) (Figure 1). Both are strikingly different, the flat-slab segment is currently amagmatic and topographicaly higher, and includes different morphostructural units, the Precordillera and the broken foreland, which comprises a series of basement block uplifts (Ramos et al., 2002). On the other hand, the normal subduction segment is characterized by an active magmatic arc, a lower Main Cordillera and a less-developed broken foreland (Giambiagi et al., 2012). The Aconcagua region straddles both segments together with the Frontal Cordillera, constituting one of the best examples of the interplay between deep and shallow deformational processes along the Andes (Giambiagi and Ramos, 2002; Giambiagi et al., 2015).

Ramos (1985a), Ramos (1988) defined the structure of the Aconcagua region as a typical thin-skinned fold-thrust belt (FTB), constituting together with the Precordillera (Allmendinger et al., 1990; Von Gosen, 1992) an exception in the Southern Central Andes, where thick-skinned tectonics is dominant (Figure 1B). However, deformation mechanisms such as normal fault inversion have been described in the southern sector of the Aconcagua FTB at 33°30°S (Giambiagi et al., 2003a). Although tectonic inversion and basement deformation have been hinted in the northern Aconcagua FTB at 32°50S (Cegarra and Ramos, 1996; Vicente and Leanza, 2009), the lack of integrative analysis of the structural setting has led to its reinterpretation as a shallow secondary feature (Armijo et al., 2010; Riesner et al., 2019). Moreover, despite recent radiometric ages and geological observations have revealed several stratigraphic inconsistencies (Vicente, 2005; Vicente and Leanza, 2009; Mackaman-Lofland et al., 2019; Martos et al., 2022; Scazziota et al., 2022; Morel et al., 2023), these new findings have not been incorporated into some of the most recent maps of the area (Riesner et al., 2018; Carrapa et al., 2022).

The objective of the present work is to revisit the classical Río Cuevas section in the Aconcagua region (32°50S), where the stratigraphy and structures are well exposed, but their low accessibility has hindered efforts to make substantial advances in its geological understanding since the work of Ramos et al. (1996a). With this objective in mind, we employed several field seasons, went through a thorough review of previous works and performed four new U-Pb detrital zircon datings, which helped to reevaluate the spatial distribution of the outcropping units, the structural mechanisms involved and the cross-cutting relationships constraining deformational events. As a result, we generated an updated geological map and a schematic cross-section where we assess the structural styles and deformational stages along the belt.

1.1 Tectonic setting of the Aconcagua FTB

The Cuevas river headwaters are located along the international limit between Chile and Argentina, running across the study area draining the Jurassic to Miocene sedimentary deposits and volcanic rocks exposed in the Aconcagua FTB (Figure 1C). This river converges with the Tupungato and Vacas rivers in the western flank of the Frontal Cordillera, giving birth to the Mendoza river (Figure 1C). To the east, the limit between the Aconcagua FTB and the Neo-Proterozoic to Triassic rocks of the thick-skinned Frontal Cordillera (Giambiagi et al., 2014) is represented by the thin-skinned Penitentes thrust (Figure 1C) (Cegarra and Ramos, 1996; Vicente and Leanza, 2009). To the West, the El Fierro fault zone separates the Aconcagua FTB from the upper Eocene to Miocene igenous rocks of the West Andean FTB (Piquer et al., 2015; Riesner et al., 2017; 2018). These three morphostructural units constitute the Andean Cordillera at these latitudes, a bivergent orogenic wedge (Ramos et al., 2002; Giambiagi et al., 2003b; Armijo et al., 2010; Farías et al., 2010). The Pocuro fault zone (Taucare et al., 2022) and the La Carrera fault system (Giambiagi et al., 2014) represent the western and eastern limits, respectively, of the Andean range at the latitudes of the study area, separating it from the Quaternary Central Valley in Chile (Farías et al., 2008) and the Miocene Cacheuta basin in Argentina (Buelow et al., 2018) (Figure 1C).

The onset of deformation in the Aconcagua FTB is nowadays considered as early Miocene in age due to the presence of Miocene synorogenic deposits in the footwall of the frontal Penitentes thrust and an important angular unconformity between highly deformed

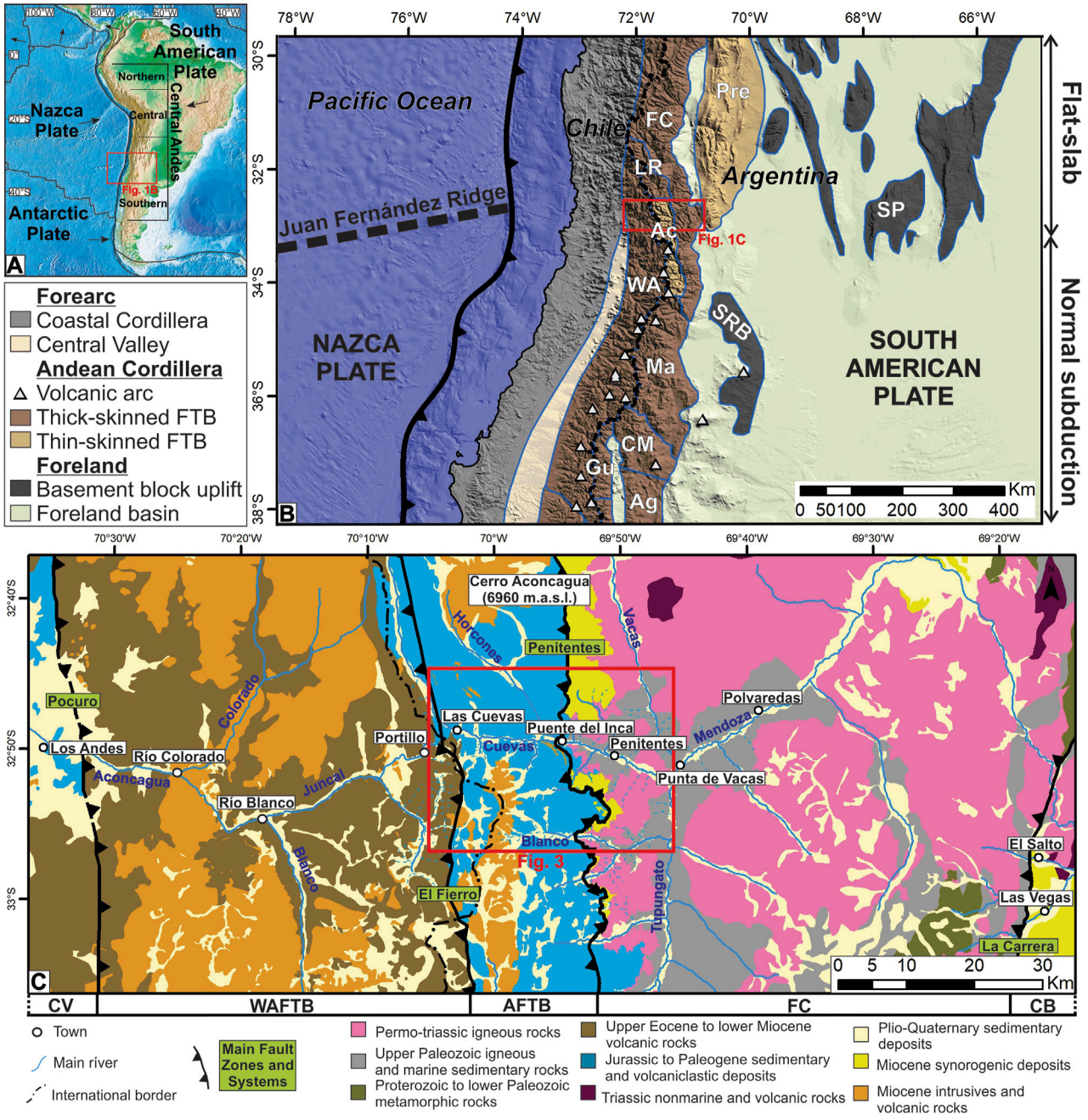

FIGURE 1
(A) Tectonic setting of the Andes following subdivisions by Ramos (1999). **(B)** Morphostructural units of the Southern Central Andes, with the study area in the northern Aconcagua FTB developed entirely over the Chilean-Pampean flat subduction segment. Abbreviations are as follows: FC, Frontal Cordillera; Pre, Precordillera; SP, Sierras Pampeanas; LR, La Ramada FTB; Ac, Aconcagua FTB; WA, West Andean FTB; Ma, Malargüe FTB; SRB, San Rafael Block; CM, Chos Malal FTB; Gu, Guañacos FTB; Ag, Agrio FTB. **(C)** Simplified geological map across the Andean orogen at the latitudes of the Cuevas River in west-central Argentina based on Rivano et al. (1993), Ramos et al. (1996a, 2010), Giambiagi et al. (2014), Piquer et al. (2015) and data from this work. Abbreviations are as follows: CV, Central Valley; WAFTB, West Andean FTB; AFTB, Aconcagua FTB; FC, Frontal Cordillera; CB, Cacheuta basin.

Mesozoic deposits and subhorizontal early to middle Miocene volcanic rocks (Cegarra and Ramos, 1996; Vicente, 2005). Important volcanic activity took place in the Aconcagua region during the middle Miocene (Ramos et al., 1996b), due to the expansion of the magmatic arc previously located in Chilean territory (Deckart et al., 2005; Montecinos et al., 2008; Piquer et al., 2015). Shortening continued during this stage, finally ceasing together with magmatism in the late Miocene when, due to the shallowing of the Nazca oceanic plate, the orogenic front migrated east to the Frontal Cordillera and the locus of the volcanic arc shifted towards the Sierras Pampeanas (Ramos et al., 2002). However, recent thermochronological studies indicate that the Frontal Cordillera at these latitudes was exhumed in early to middle Miocene times (Hoke et al., 2015; Lossada et al., 2020a),

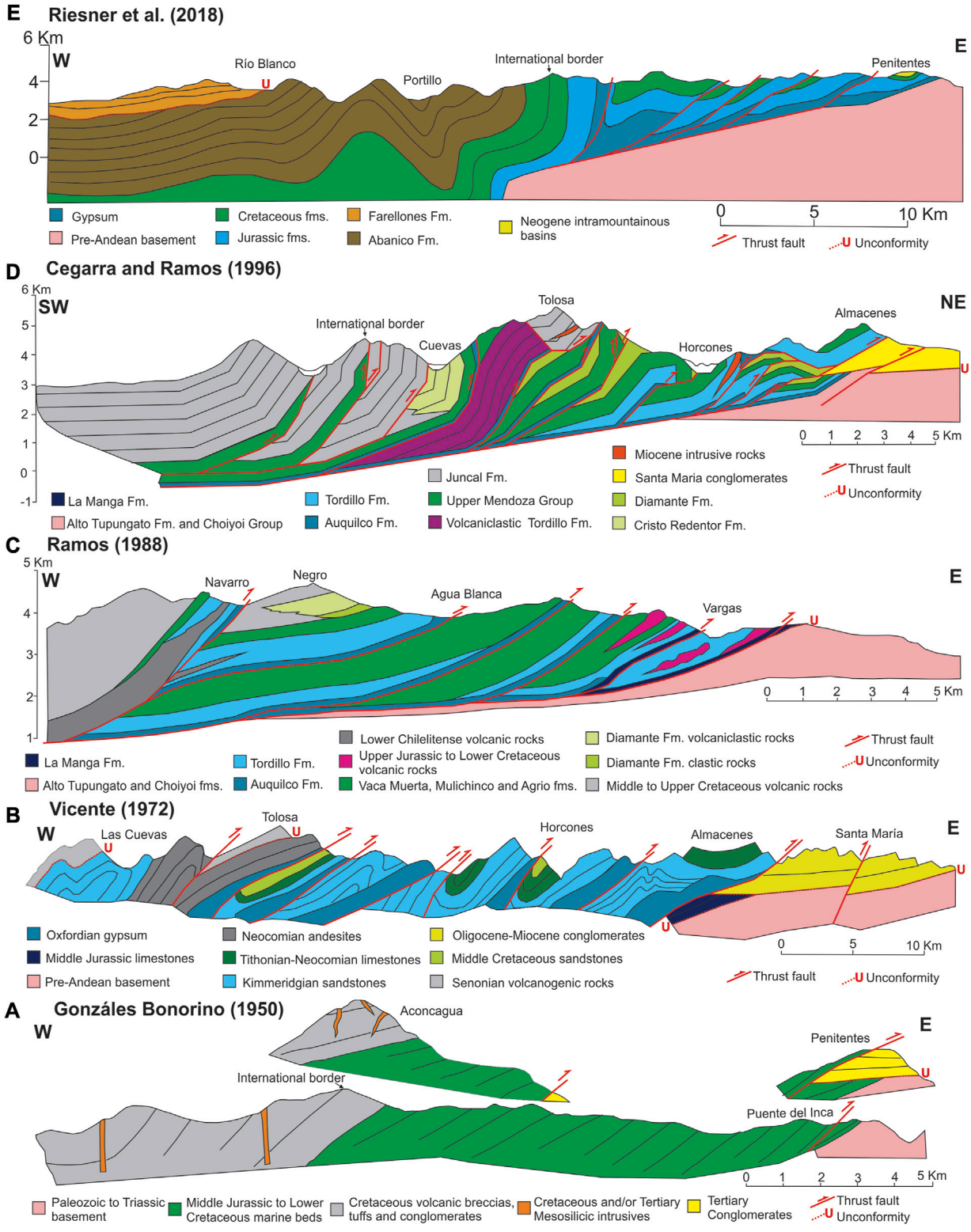

FIGURE 2
Evolution of structural sections along the Cuevas River showing the advances in the geological knowledge and different interpretations for the structure and cross-cutting relationships. **(A)** Gonzáles Bonorino (1950). **(B)** Vicente (1972). **(C)** Ramos (1988). **(D)** Cegarra and Ramos (1996). **(E)** Riesner et al. (2018).

converting the final stage of shortening in the Aconcagua FTB in an out-of-sequence deformational phase (Martos et al., 2022). These challenging models propose that the exhumation of the Frontal Cordillera precedes the activity in the Aconcagua FTB, in opposition to the classical eastern vergence model of Andean mountain building (Riesner et al., 2019). Furthermore, although evidence of

pre-Miocene deformation in the Aconcagua FTB has existed in the literature for more than a century (Schiller, 1912; Vicente et al., 1973; Orts and Ramos, 2006), the lack of comprehensive geological studies has prevented the evaluation of older orogenic phase proposals. Therefore, to track the origin of these proposals, we will review some of the key highlights in the geological knowledge of the region.

1.2 Evolution of the geological knowledge in the Aconcagua region

The first geological expedition into the Aconcagua region was the incursion of Charles Darwin across the Andes in 1835 (Darwin, 1846). Throughout his trip along the Cuevas River he described limestones containing Early Cretaceous marine fossils, along with andesites, conglomerates, sandstones and gypsum deposits. He also performed the first schematic section along the Cuevas River, which consisted of thousands of meters of west-dipping strata affected by several dislocations. It took almost 80 years until the first systematic observations performed by Schiller (1912) were published, showing the presence of Jurassic and Cretaceous rocks affected by a series of low-angle reverse faults he denominated thrusts. Schiller (1912) described the easternmost thrust located in Puente del Inca in detail, where Tertiary conglomerates sitting unconformably over upper Paleozoic to Lower Cretaceous rocks are overthrust by Middle Jurassic to Lower Cretaceous deposits. In his work, Schiller (1912) presents a series of structural sketches, where he emphasizes the presence of an angular unconformity between Upper Cretaceous volcanic rocks and Lower Cretaceous marine deposits, in what he considers an evidence of a Late Cretaceous tectonic event.

The first structural section along the Cuevas River was published by Gonzáles Bonorino (1950), where he shows 5 km of unrepeated west-dipping (30°) monoclinal Middle Jurassic to Lower Cretaceous marine strata (Figure 2A). West of the international border, he shows that these sequences are overlain by volcanic breccias, tuffs and conglomerates of apparent Cretaceous age penetrated by Cretaceous and/or Tertiary mesosilicic intrusives, which he describes as the main constitutents of the Cerro Aconcagua (Figure 2A). In his section, Gonzáles Bonorino (1950) only recognizes the frontal low-angle thrust fault described by Schiller (1912) in Puente del Inca, which he hypothesizes as one of the main responsibles for the high elevation of the Cerro Aconcagua. A year later, the first geological map of the Aconcagua region was published (Groeber, 1951), but it took ten more years until the publication of the first geological map and structural observations of the neighbouring Chilean territory performed by Aguirre Le Bert (1960).

The following breakthrough in the geological knowledge of this area is represented by the work of Vicente (1972), who added several thrusts detaching over gypsum levels, following the initial proposal of Schiller (1912) (Figure 2B). A higher detail is observed in the stratigraphy along the section, which highlights the presence of two unconformities: one at the base of the Tertiary conglomerates and the other one between an Upper Cretaceous volcanogenic unit and the underlying Mesozoic beds, attributing the latter as an evidence of a Late Cretaceous contractional phase (Vicente et al., 1973). In parallel, Yrigoyen (1972, 1976, 1979) compiled all the information available and added his own observations, which led him to propose that at least six different orogenic phases affected the Aconcagua region, the main one being the one that occurred during the Cretaceous. However, a couple of years later, Munizaga and Vicente (1982) present one of the first radiometric datasets for this area, showing that most of the volcanic outcrops above the angular unconformity exhibit late Oligocene to Miocene ages, undermining the role of Cretaceous contraction in this area.

Ramos (1985a; 1988) built the first balanced structural cross-sections south of the Cuevas River, proposing a main *décollement* in the Oxfordian gypsum deposits (Auquilco Formation), with the exception of the frontal Penitentes thrust in the Vargas creek, where the structure detaches in the Callovian limestones (La Manga Formation) (Figure 2C). In this last area, Ramos (1985b) recognized the presence of volcanic intercalations in the Upper Jurassic nonmarine red beds (Tordillo Formation), which were correlated with the volcaniclastic sequences (Lower Chilelitense) exposed in the inner sector of the Aconcagua FTB (Figure 2C) (Ramos, 1985b; 1988; Sanguinetti, 1989). Ramos (1985b) also identified a lower clastic and an upper volcaniclastic section in the Lower Cretaceous red beds (Diamante Formation), conformably overlain by a thick sequence of Middle to Upper Cretaceous volcanic rocks, which lead him to propose that the main contractional phases in the Aconcagua FTB occurred afterwards, during Eocene and Miocene times.

A series of observations performed by Sanguinetti and Cegarra (1991) near the Cuevas River headwaters confirmed the great thickness increase in the Upper Jurassic nonmarine sequences between the frontal and the inner sectors of the belt hinted in previous works (Yrigoyen, 1972; 1976; 1979; Ramos, 1985b). This fact was taken into account by Cegarra and Ramos (1996) in their structural cross-section of the northern margin of the Cuevas River, where they interpret the presence of a Late Jurassic half-graben in the inner western sector, filled by the Upper Jurassic volcaniclastic sequences (Tordillo Formation) (Figure 2D). These authors claim that deformation in this area began in the early Miocene with the inversion of the half-graben, continued by thin-skinned deformation during the middle Miocene and ended with the activity of a frontal structure, rooted into the basement, which offsets the Miocene conglomerates (Figure 2D). In their model, they included the refinement of the Cretaceous stratigraphy of Cristallini and Ramos (1996), showing the presence of volcanic rocks (Juncal Formation) in the inner sector grading eastwards to volcaniclastic (Cristo Redentor Formation) and sedimentary deposits (Diamante Formation) (Figure 2D). The deposition of the Miocene conglomerates (Santa Maria), coeval with the emplacement of the trachytic intrusives in Cerro Tolosa and Horcones areas, suggests a hiatus during the Paleogene (Figure 2D).

The most recent developments in the Aconcagua region were promoted by the dating of several volcanic units outcropping in Chilean territory (Gana and Wall, 1997; Fuentes et al., 2002; Nyström et al., 2003; Deckart et al., 2005; Montecinos et al., 2008; Piquer et al., 2015), showing that most of the rocks assigned to the Cretaceous (Juncal Formation, Ramos et al., 1996a) presented upper Eocene to lower Miocene ages. This motivated their reassignation as part of the Abanico and Farellones formations, being the former interpreted as the infill of an extensional intra-arc basin, and the latter as the synorogenic

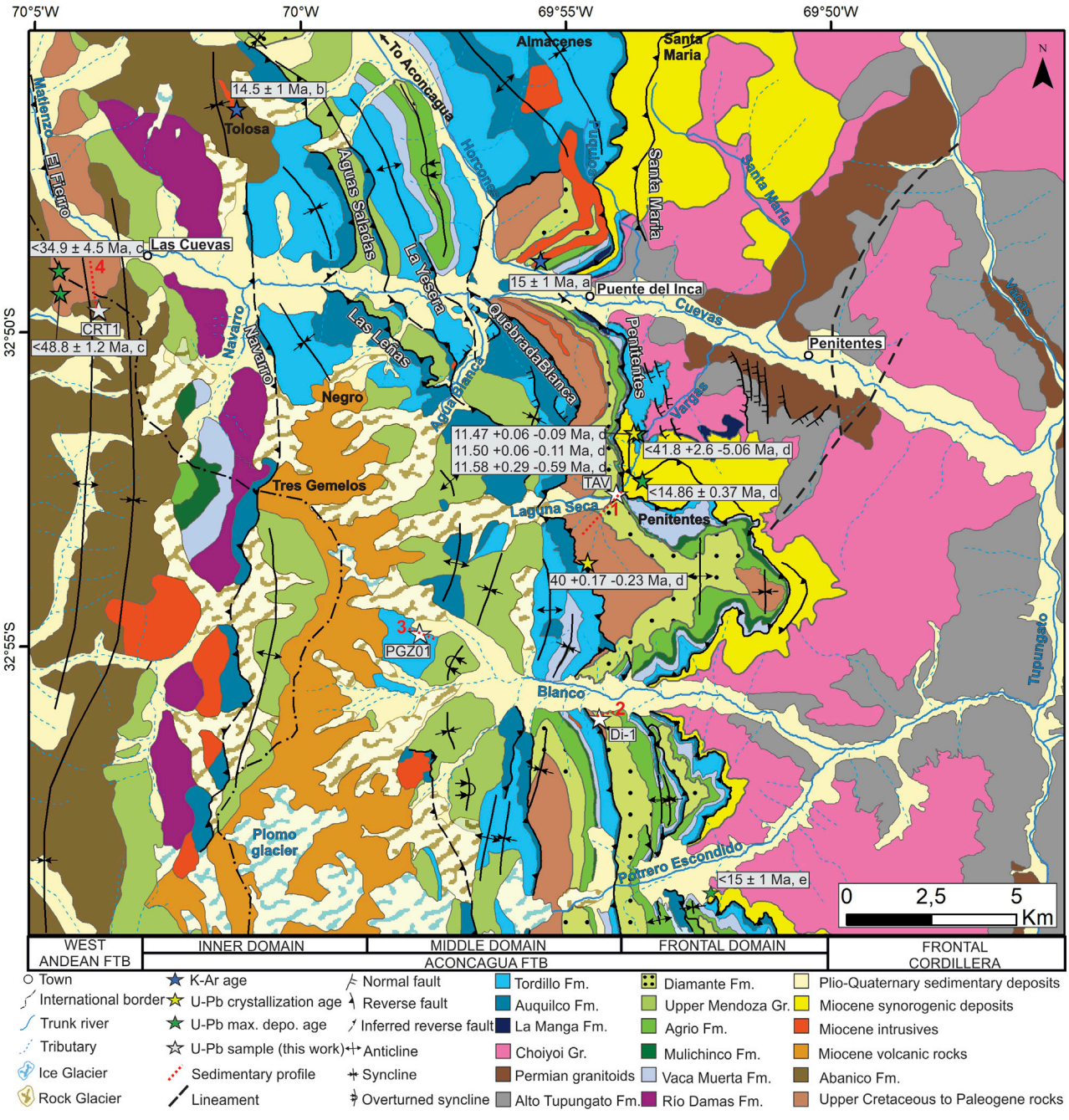

FIGURE 3
Geological map of the Aconcagua region between the Cuevas river and Potrero Escondido creek showing the location of the radiometric ages and the new sedimentary profiles performed in this work. Main rivers, creeks and glaciers are labeled in blue, mountains in black and reverse faults in white. The reference for the ages are as follows. 1. Munizaga and Vicente (1982), 2. Ramos et al. (1996a), 3. Mackaman-Lofland et al. (2019), 4. Carrapa et al. (2022), 5. Martos et al. (2022).

deposits of an early Miocene contractional event, evidenced by the unconformable relation between both units (Charrier et al., 2002; Fock et al., 2006). In this line, Armijo et al. (2010) and Riesner et al. (2017, 2018) defined the West Andean FTB, composed by several long-wavelength, asymmetric, west-vergent folds located west of the international border (Figure 2E). These authors constrained its onset of deformation to 25–20 Ma based on the age of the unconformity between Abanico and Farellones formations, indicating it occurred before the initiation of shortening in the Aconcagua FTB, which was reinterpreted as a secondary feature in the Andes.

The geological map of the Aconcagua FTB has not suffered any major modifications since its publication by Ramos et al. (1996a). However, motivated by the great amount of new radiometric ages in Chile, Vicente (2005) reanalyzed the angular unconformity capping the deformed Mesozoic sedimentary deposits described in Schiller (1912) and Vicente

et al. (1973), obtaining a middle to late Miocene age for the upper volcanic unit. During his revisit to the eastern frontal sector, he also detected two distinct Miocene units, proposing their division in Penitentes Conglomerates and Santa Maria Volcanic Agglomerates. These observations led Vicente (2005) to favor the early Miocene as the main deformational phase in the area, although he highlighted the effects of the Eocene and Late Cretaceous events, being the latter afterwards supported by the description of growth strata in Cretaceous red beds (Diamante Formation, Orts and Ramos, 2009). Vicente and Leanza (2009) continued with the revisiting of the frontal area in the Vargas creek, proposing a detachment in Upper Jurassic near-shore limestones for the Penitentes thrust, identifying a series of non-inverted Late Jurassic half-grabens and documenting a frontal thick-skinned reverse fault. More recently, Mackaman-Lofland et al. (2019) dated detrital zircons from the Cristo Redentor Formation in its type locality, the international border, and obtained Eocene maximum depositional ages, challenging its Cretaceous assignation (Cristallini and Ramos, 1996).

2 Methodology

The several inconsistencies in the stratigraphy, the outdated geological maps and the contradicting proposals regarding the structure and deformational timing motivated us to revisit the Aconcagua region to perform new geological and structural observations between the Cuevas river and the Potrero Escondido creek to the south, aided by sedimentological studies and geochronological analyses. During this visit we examined the area between the frontal eastern sector of the Aconcagua FTB and the international border analyzing the relation between the different geological units, taking into consideration the most recent developments in the region. Due to its great outcrop exposure, we inspected the geology above the Penitenites thrust in the Vargas creek, where we performed a complete sedimentary profile and obtained a sample for U-Pb detrital zircon dating (TAV). Two additional profiles along with two U-Pb detrital zircon ages (Di-1 and PGZ01) were performed along the Blanco River valley (Figure 3), targeting red beds whose previous mapping presented discrepancies with our new observations. Given the recent age reassignation of the Cristo Redentor Formation, we inspected its type locality in the inner sector, where we obtained a sample from a tuff intercalated in the upper volcanic unit for zircon U-Pb dating (CRT1). Considering all the new ages and observations, together with the data provided by other authors, we were able to update the stratigraphy of this area, which was used to reinterpret cross-cutting relationships, create an updated geological map and build a schematic cross-section.

Samples TAV and CRT1 were processed for U-Pb zircon dating at the Laboratory of La.Te.Andes S.A (Salta, Argentina), where concentration of heavy minerals and separation of zircons grains were done by standard techniques. After separation, one hundred grains were placed on epoxy mounts and polished to approximately half-thickness, which were afterwards analyzed and dated by U-Pb LA-ICP-MS (Laser Ablation Inductively Coupled Plasma Mass Spectrometry). On the other hand, detrital zircons from samples Di-1 and PGZ01 were concentrated in the Instituto de Geocronología y Geología Isotópica (INGEIS, Univerisdad de Buenos Aires—CONICET) by standard techniques of heavy mineral separations. After separation, approximately 120 grains were placed on epoxy mounts, polished and cleaned with 3% nitric acid before analysis and dated by U-Pb (LA-MC-ICP-MS). A complete list of the analytical data and details of the methodology used in both laboratories can be found in the Supplementary Material. To determine the maximum depositional age, we used the youngest single cluster overlapping at 2σ uncertainty and calculated a weighted mean $^{206}Pb/^{238}U$ age (Gehrels, 2014). U-Pb ages were plotted in frequency histograms and KDE diagrams (Kernel Density Estimation) to analyze the source areas of sediments, using the software *Isoplot* (Ludwig, 1999) and *IsoplotR* (Vermeesch, 2018).

3 Results

3.1 Updated stratigraphy and geological map of the Aconcagua region

The oldest rocks in the study area are exposed immediately to the east of the Aconcagua FTB in the Frontal Cordillera, represented by the Carboniferous Alto Tupungato Formation, Permian granitoids and Permo-Triassic volcanic rocks of the Choiyoi Group, which constitute the stratigraphic basement of the Aconcacua basin (Pérez and Ramos, 1996) (Figure 3). The Aconcagua basin started to develop in Middle Jurassic times with the deposition of fossiliferous limestones assigned to the La Manga Formation, which represent the first marine transgression in the area (Lo Forte, 1996) (Figure 4). A marine regression took place in Late Jurassic times, evidenced by the presence of gypsum deposits of the Auquilco Formation, followed by the volcanic and volcaniclastic emplacement of the Río Damas Formation, which crops out in the western sector of the study area (Aguirre Le Bert, 1960) (Figure 3). Towards the east, the volcanic and volcaniclastic Río Damas Formation transitions into the nonmarine red beds of the Tordillo Formation, which covers unconformably the Auquilco Formation and represents the beginning of the sedimentation of the Mendoza Group in this region (Lo Forte, 1996; Acevedo et al., 2020) (Figure 4). The rest of the Mendoza Group is constituted by the Vaca Muerta, Mulichinco and Agrio formations, represented mainly by black shales, sandstones and carbonates, respectively, deposited between Late Jurassic and Early Cretaceous times (Aguirre-Urreta and Lo Forte, 1996) (Figure 4). In Ramos et al. (1996a), volcanic levels were mapped interbedded with the red beds of the Tordillo Formation, included under the denomination of Volcanitas Vargas (Figure 4). Besides, a series of volcanic lenses were also reported as intercalated with the Vaca Muerta and Mulichinco formations, assigned to the Volcanitas Laguna Seca (Ramos et al., 1996b) (Figure 4).

Among the main modifications in the map of the study area is the reinterpretation of the outcrops of the Mendoza Group in

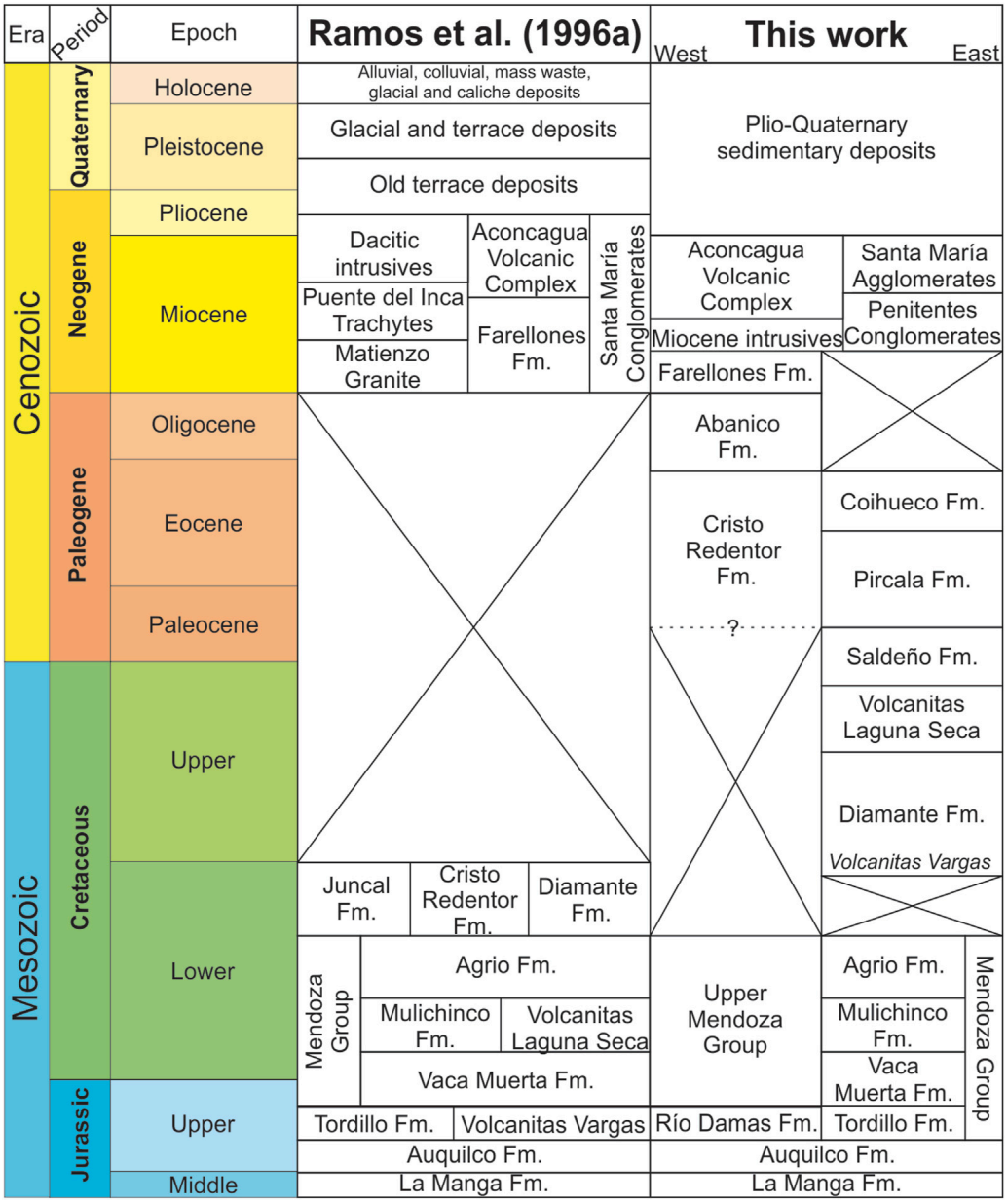

FIGURE 4
Previous stratigraphic arrangement in the Aconcagua region proposed by Ramos et al. (1996a) compared to the stratigraphic column proposed in this work.

the Vargas and Laguna Seca creeks (Figure 3), which had been previously mapped as the La Manga Formation (Ramos et al., 1996a; Vicente and Leanza, 2009), and the stratigraphic position of their volcanic intercalations (Figure 4). New field data and U-Pb zircon dating (see following sections) indicate that the Volcanitas Vargas are part of the basal section of the Upper Cretaceous Diamante Formation, whereas the Volcanitas Laguna Seca correspond to a separate and new informal unit of probable latest Cretaceous age overlying the Diamante Formation (Figure 4). In our new map, the outcrops of the Upper Mendoza Grup are restricted in thickness and, while their age in this frontal sector is well constrained to the Tithonian-Hauterivian by ammonite fossils (Aguirre-Urreta and Lo Forte, 1996; Vicente and Leanza, 2009; Vennari, 2016), its sedimentary facies are atypical and highly condensed. South of this area, in the Blanco river, Morel et al. (2023) described an erosive unconformity separating the uppermost Agrio Formation from the overlying Diamante Formation (Figure 4). In order to confirm our new mapping and constrain the duration of the hiatus represented by the unconformity between both formations, a U-Pb sample was taken from the base of the Diamante Formation in the Vargas Creek (TAV in profile 1, Figure 3; Figure 5).

The analysis of the Diamante Formation was complemented by a profile logged in a sequence of red beds exposed in the Blanco River valley, previously assigned to the Mulichinco

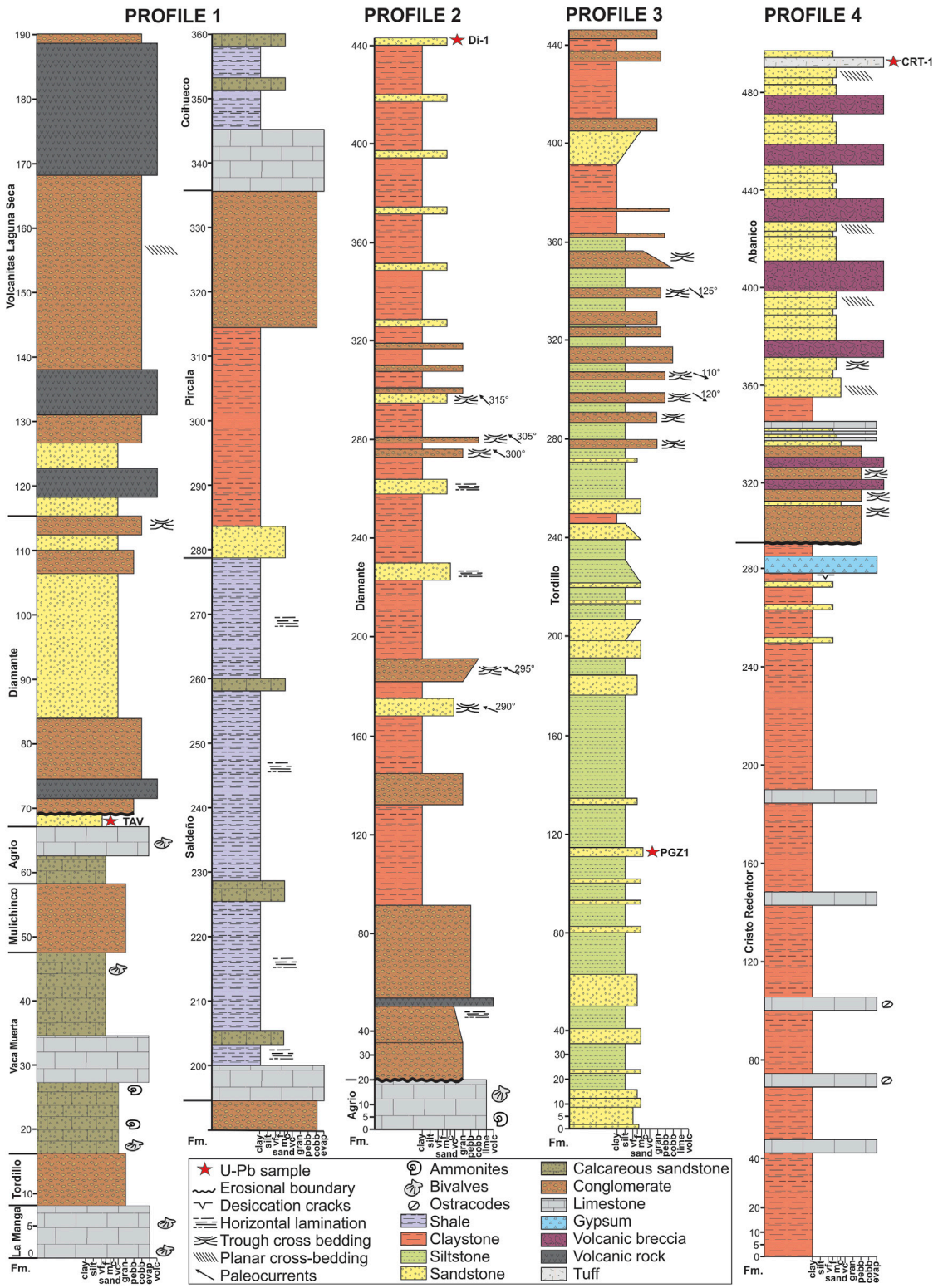

FIGURE 5
Sedimentary profiles performed in the study area and location of the U-Pb detrital zircon samples (for map location see Figure 3). Profile 4 is modified from Cristallini and Ramos (1996).

Formation (Ramos et al., 1996a). We obtained an Upper Cretaceous U-Pb detrital zircon maximum depositional age that confirms this outcrops assignation as the Diamante Formation (Di-1 in profile 2, Figure 3; Figure 5). To the west, previous mapping at the headwaters of the Blanco river showed nonmarine red beds of the Diamante Formation

overlain by the volcanic and volcaniclastic rocks of the Juncal Formation (Ramos et al., 1996a). A recent Ar-Ar age obtained from the outcrops of the Juncal Formation revealed a late Miocene age, suggesting that this volcanism corresponds to the younger Aconcagua Volcanic Complex (Scazziota et al., 2022). With this in mind, we performed a sedimentary profile and a U-Pb zircon dating on the red beds, previously assigned to the Diamante Formation (PGZ01 in profile 3, Figure 3; Figure 5). We obtained a Late Jurassic age, which corroborates the proposal of Vicente et al. (1973) that assigned these sequences to the Tordillo Formation.

Given the younger ages obtained from several volcanic outcrops mapped as the Cretaceous Juncal Formation, we revisited one of the profiles of Cristallini and Ramos (1996) in the surroundings of the Chilean-Argentinian border. Previous maps in the area show that the Juncal Formation rests upon the outcrops of the Upper Mendoza Group and is also thrusted over the Cristo Redentor Formation (Ramos et al., 1996a). The age of the Cristo Redentor Formation, previously considered as a lateral equivalent of the Cretaceous Diamante and Juncal formations (Cristallini and Ramos, 1996), was recently reassigned to the late Paleogene based on a series of new U-Pb detrital zircon maximum depositional ages (Mackaman-Lofland et al., 2019) (Figure 3; Figure 4). We performed a sedimentary profile along the contact between the Cristo Redentor Formation and the overlaying volcanic unit, and obtained an U-Pb zircon crystallization age at the top of the section (CRT1 in profile 4, Figure 3; Figure 5). This analysis yielded a late Eocene age, which indicates that this volcanic unit corresponds to the Abanico Formation, and also confirms the age reassignation for the Cristo Redentor Formation. These ages suggest that a hiatus separates the Cristo Redentor Formation from the Lower Cretaceous Upper Mendoza Group in the western Aconcagua FTB (Figure 3; Figure 4).

As mentioned before, we redefined the stratigraphy of the Laguna Seca and Vargas creeks in the frontal sector of the Aconcagua FTB where over the Diamante Formation, and above the Volcanitas Laguna Seca, a sedimentary sequence crops out, which we interpret as partly coeval with the Cristo Redentor Formation from the inner sector of the Aconcagua FTB. Our sedimentological analyses (see section 3.3.2) revealed that these rocks can be correlated with the Saldeño, Pircala and Coihueco formations, a series of Maastrichtian to middle Eocene sedimentary units that have been described south of the study area (Giambiagi et al., 2003a; Tunik, 2003; Horton et al., 2016). These outcrops had been previously mapped as the Vaca Muerta, Mulichinco and Agrio formations, despite the absence of diagnostic fossils (Sanguinetti, 1989; Ramos et al., 1996a), although our data indicate that these rocks correspond to younger units, in agreement with Morel et al. (2023). Noteworthy, a zircon U-Pb age of 40 Ma was adscribed to a sill cutting the Agrio Formation in this sector (Carrapa et al., 2022) that, considering our new interpretation, could in turn correspond to a volcanic or subvolcanic rock emplaced during the sedimentation of the Coihueco Formation (Figure 3).

The upper Paleogene and Neogene stratigraphy of this region was redefined on the basis of on the recent ages obtained from volcanic sequences close to the international border (Piquer et al., 2015; Scazziota et al., 2022 and this work), and from sedimentary deposits and volcanic rocks located in the frontal sector of the Aconcagua FTB (Vicente, 2005; Carrapa et al., 2022; Martos et al., 2022) (Figure 3). These new ages indicate that the volcanic sequences exposed in the inner sector of the Aconcagua FTB correspond to the upper Eocene-lower Miocene Abanico and Farellones formations (Figure 3; Figure 4). The stratigraphy continues with a series of miocene intrusives associated with the activity of the Aconcagua Volcanic Complex (15–8 Ma, Ramos et al., 1996b), whose outcrops are found only in Argentine territory (Figure 3; Figure 4). The deposition of sedimentary rocks in the frontal sector of the Aconcagua FTB occurred coeval to this volcanic event, and can be divided into the Penitentes Conglomerates (15–12 Ma) and the Santa Maria Volcanic Agglomerates (12–8 Ma) (Vicente, 2005; Carrapa et al., 2022; Martos et al., 2022) (Figure 3; Figure 4). Finally, since magmatism in the study area ceased in the late Miocene, Plio-Quaternary sequences are completely sedimentary, characterized by glacial, fluvial, alluvial, caliche and mass-waste deposits (Figure 3; Figure 4).

3.2 New geochronological data

A total of 105 zircons were analyzed from sample PGZ01, although 17 were discarded due to high analytical error or high ^{204}Pb content. The remaining 88 ages are distributed in 5 different peaks: *ca*. 288 Ma, 257 Ma, 229 Ma, 184 Ma and 150 Ma (Figure 6). We calculated a maximum depositional age of 150.78 ± 0.55 Ma for this coarse-grained sandstone based on the 4 youngest grains whose ages overlap at the 2σ uncertainty (Figure 6), suggesting that the red beds outcropping in the Blanco River headwaters correspond to the Upper Jurassic Tordillo Formation (Figure 3 and profile 3 in Figure 5).

Fifty-five analyses were done for sample TAV, but only forty-two presented concordant ages. The KDE plot shows a polymodal distribution with a greater peak at *ca*. 278 Ma, younger subordinate peaks at *ca*. 161 Ma and 214 Ma, older subordinate peaks between 358 Ma and 2,136 Ma, and a single grain representing the youngest age of 96 ± 6 Ma (Figure 6). Despite not being able to calculate a maximum depositional age (following Dickinson and Gehrels, 2009), the age of the youngest detrital zircon agrees with our interpretation that the fine-grained sandstones from where it was obtained are part of the Upper Cretaceous Diamante Formation (Figure 3 and profile 1 in Figure 5).

Di-1 corresponds to a sandstone sample obtained from the top of the sequence of red beds laterally equivalent to the ones from where we obtained the sample TAV (Figure 3). 108 zircons were analyzed, but only 98 presented reliable ages, ranging between 92 Ma and 2,631 Ma (Figure 6). The distribution of these ages show a main peak at *ca*. 245 Ma and subordinated peaks at *ca*. 93 and 144 Ma, as well as Cambrian and Mesoproterozoic peaks. A weighted mean age of 93.51 ± 0.21 Ma was calculated using the 3 youngest zircon ages (Figure 6), confirming our assignation of these red beds as part of the Upper Cretaceous Diamante Formation (Figure 3 and profile 2 in Figure 5).

One hundred and seven zircons were analyzed from the tuff sample CRT1, but only fifty-seven presented concordant ages.

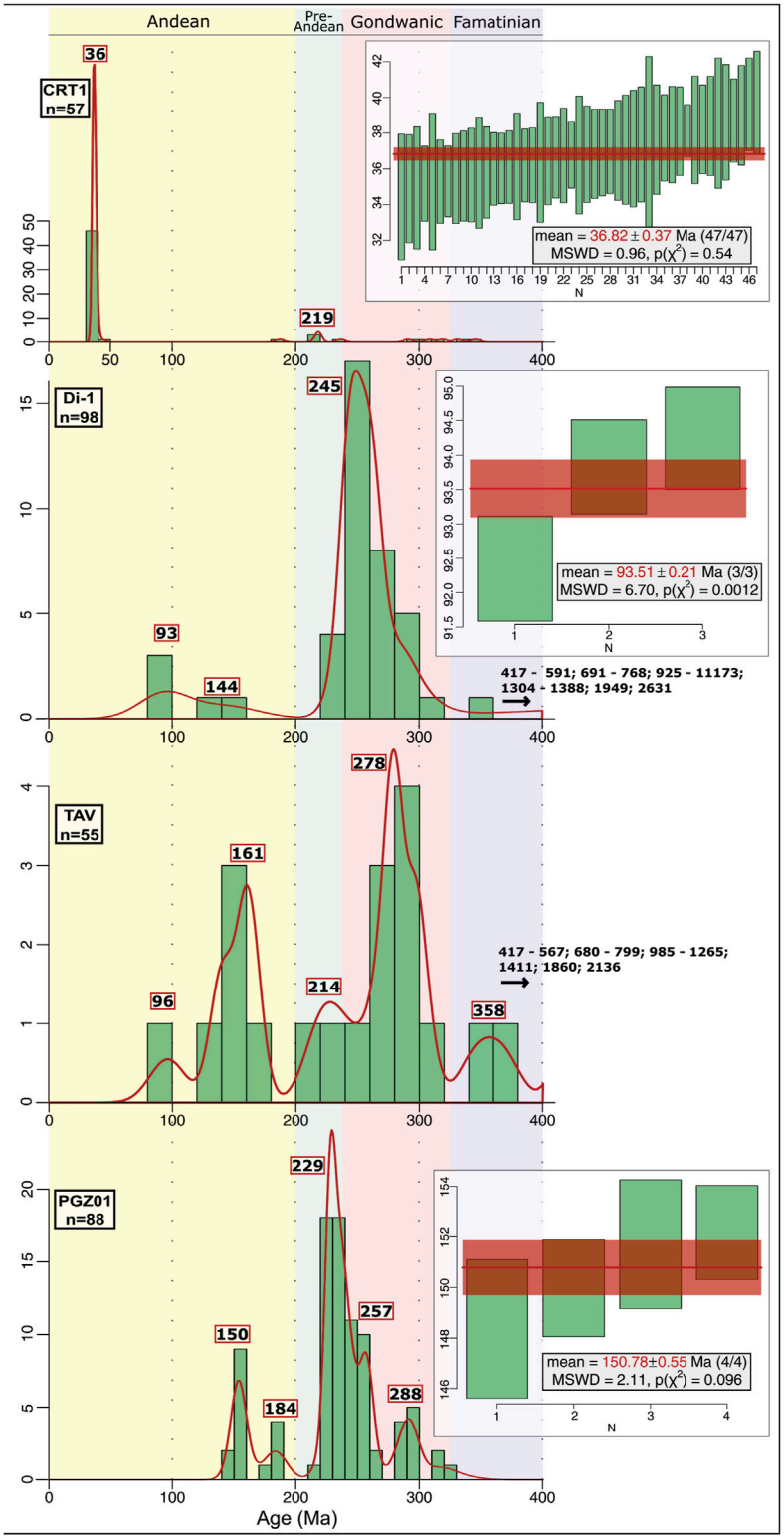

FIGURE 6
Frequency histograms and KDE plots of the U-Pb ages of detrital zircons younger than 400 Ma obtained from a series of samples taken from key units distributed along the study area (see Figure 3; Figure 5). A weighted mean $^{206}Pb/^{238}U$ age was calculated using the youngest zircon cluster whenever the sample presented three or more ages overlapping in the 2σ uncertainty.

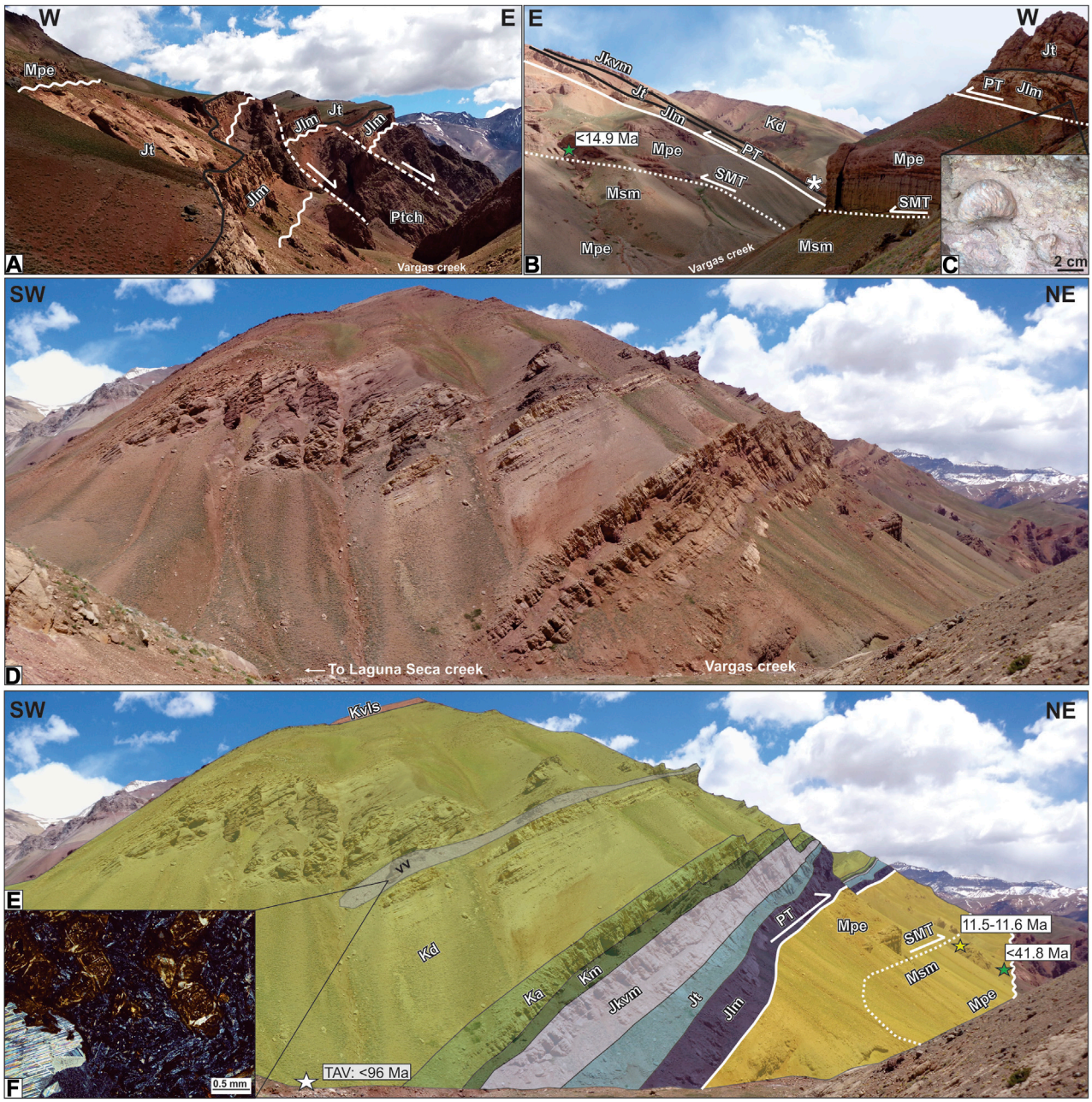

FIGURE 7
(A) Normal faults in the foot-wall of the Penitentes thrust affecting the La Manga Formation (Jlm) and Choiyoi Group (PtCh), producing a series of half-grabens filled with the Tordillo Formation (Jt) and unconformably overlain by the Penitentes Conglomerates (Mpe). **(B)** The Santa Maria thrust (SMT) is observed in both margins of the Vargas creek, placing the Penitentes Conglomerates over the Santa Maria Volcanic Agglomerates (Msm). The Penitentes thrust (PT) in this creek detaches in the limestones of the La Manga Formation, confirmed by its fossiliferous content. The asterisk marks the position of the ammonite fossils described by Vicente and Leanza (2009) in the Vaca Muerta Formation (Jkvm), which are found above the limestones here identified as the La Manga Formation. **(C)** Oyster fossils, identified as Aetostreon, typical of the La Manga Formation. **(D,E)** A sedimentary profile logged in the valley floor and the age obtained from sample TAV helped us identify the Mesozoic units above the Penitentes thrust, including the reassignation of the Volcanitas Vargas (vv) as part of the Diamante Formation, and the designation of the Volcanitas Laguna Seca as a new and informal unit (Km is Mulichinco Formation, Ka is Agrio Formation, Kd is Diamante Formation and Kvls are the Volcanitas Laguna Seca). **(F)** The Volcanitas Vargas under the microscope correspond to a porphyritic basalt, showing olivine phenocrysts (replaced by iddingsite) in an intersertal groundmass.

The KDE diagram of U-Pb ages shows that the main peak is located at *ca.* 36 Ma, with the presence of a subordinate peak at *ca.* 219 and disperse single ages between 291 Ma and 346 Ma (Figure 6). We obtained a weighted mean age of 36.82 ± 0.37 Ma considering the fourty-seven younger ages that overlap at the 2σ uncertainty (Figure 6). Based on the lithology and stratigraphic position of the sample, we interpret this as a crystallization age from a tuff intercalated in the base of the upper Eocene to Oligocene Abanico Formation (Figure 3 and profile 4 in Figure 5).

3.3 New geological and structural observations between the Cuevas and Blanco river valleys

The updated geological map (Figure 3) and stratigraphic column (Figure 4) are not only the result of a thorough bibliographic review, the new sedimentological profiles (Figure 5) and U-Pb ages (Figure 6), but also of a large number of original geological and structural observations. In this next section we will go through some of the most representative locations between the Cuevas and Blanco rivers, which were key to help confect our map and support our interpretations.

3.3.1 The Penitentes thrust in the Vargas creek

From east to west, the first area we revisited corresponds to the Vargas Creek (Figure 7), the best location to analyze the transition between the foot-wall and hanging-wall of the Penitentes thrust (Figure 3). In the foot-wall, Ramos et al. (1996a) had mapped some minor repetitions in the La Manga Formation, which we reinterpreted as east-dipping normal faults following Vicente and Leanza (2009) (Figure 7A). These normal faults offset the crystalline basement of the Choiyoi Group and the limestones of the La Manga Formation, generating a series of half-grabens filled with the red beds of the Tordillo Formation (Figure 3; Figure 7A). The deposits of the Tordillo Formation are unconformably overlain by the Miocene Penitentes Conglomerates (Figure 7A), which grade upwards to the deposits of the Santa Maria Volcanic Agglomerates (Figure 7B). The Penitentes Conglomerates appear again on top of the Santa Maria Volcanic Agglomerates due to the presence of a reverse fault, already identified by Vicente and Leanza (2009), which we will call the Santa Maria thrust (Figure 7B). Above the Penitentes Conglomerates, the activity of the Penitentes thrust placed a Meso-Cenozoic sequence. The hanging-wall of the Penitentes thrust comprises at the base limestones rich in oyster fossils identified as *Aetostreon* (Figure 7C), an extinct subgenus within the genus *Exogyra* of the *Gryphaea* family, typical of the La Manga Formation (Bressan and Palma, 2010). This confirms the mapping of the La Manga Formation as the detachment of the Penitentes thrust in this creek (Ramos et al., 1996a), constituting a local anomaly given that this thrust detaches in the Auquilco Formation both to the north (Giambiagi et al., 2022b) and to the south (Martos et al. (2022) (Figure 3). Since Vicente and Leanza (2009) had argued in favor of a detachment in the Vaca Muerta Formation due to the presence of ammonite fossils over the Penitentes thrust, a sedimentary profile was performed in this area (profile 1 in Figure 5).

The profile begins on the valley floor with 7 m of limestones of the La Manga Formation overlain by 9 m of red conglomerates corresponding to the Tordillo Formation, which are followed by 30 m of red calcareous sandstones and white limestones of the Vaca Muerta Formation (Figure 7D; Figure 7EA), from where Vicente and Leanza (2009) collected their fossils (Figure 7B). This sequence is covered by 10 m of reddish conglomerates and 9 m of red calcareous sandstones and limestones with small bivalve fossils, which we assigned to the Mulichinco and Agrio formations, respectively (Figure 5). The succession transitions to fine-grained red sandstones from where we sampled TAV for dating, which confirmed the passage towards the Diamante Formation (Figure 7E). The sedimentary profile leaves the valley floor and moves into one of the tributaries of the Laguna Seca creek (Figure 3), where it continues with coarse-grained conglomerates interbedded with a 2-m thick volcanic rock, which had been mapped as the Volcanitas Vargas by Sanguinetti (1989) and Ramos et al. (1996a). A sample was taken from this outcrop for inspection under the petrographic microscope, showing mafic phenocrysts in a groundmass formed mostly by randomly oriented plagioclase microliths (Figure 7F). This rock presents abundant, mostly spherical, carbonate-rich amygdules that confer a white-speckled appearance and present a pervasive carbonate, oxide, chlorite, and clay alteration. Mafic phenocrysts include euhedral olivine crystals, characterized by irregular fractures, and prismatic subhedral pyroxenes, both intensely altered to ferromagnesian clays. The groundmass exhibits an intersertal assemblage of mostly plagioclase microliths, pyroxenes, opaque minerals, and interstitial clays. Therefore, we reinterpret this volcanic level as a basalt close to the base of the Diamante Formation, in agreement with the observations made by Vicente and Leanza (2009). A similar outcrop was detected in the sedimentological profile performed in the Diamante Formation in the Río Blanco valley, indicating a wide distribution for this volcanic intercalation (profile 2 in Figure 5). The Diamante Formation from both profiles is quite different in facies, provenance and thickness, since we only measured 47 m in the Laguna Seca creek, compared to the 420 m in the Río Blanco valley. While in profile 1 the lithologies are essentially sandstones and conglomerates composed by rhyolitic and quartz clasts, profile 2 consists mainly of claystones interbedded with sandy and conglomeratic lenses with horizontal lamination and trough cross-bedding (paleocurrents to the NW). In contrast, the conglomerates in this last profile also show an important clastic population of limestones, especially in the coarse-grained strata above the unconformable contact with the Agrio Formation (Figure 5).

3.3.2 The latest Cretaceous to Paleogene sequences in the Laguna Seca creek

Above the Diamante Formation in the Laguna Seca creek (profile 1 in Figure 5) shows a sudden shift in lithology and provenance with the appearance of an 80-m thick conglomeratic unit with three volcanic intercalations, which we assigned to a new informal unit: the Volcanitas Laguna Seca (Figures 8A, B). Its designation as a new unit was also motivated by differences observed in the clastic provenance observed in the conglomerates, which in the case of the Volcanitas Laguna Seca are dominated by mafic volcanic clasts, not observed in the Diamante Formation. A closer inspection of the volcanic intercalations shows that these consist of micro-porphyritic basalts with olivine phenocrysts embedded within a fine-grained groundmass (Figures 8C, D). Olivine phenocrysts are mostly altered to iddingsite and serpentine, while the groundmass shows moderate clay, carbonate, and chlorite alteration. The latter has intergranular to intersertal textures, composed of plagioclase microliths, clinopyroxenes, and opaque minerals, in some cases with interstitial clay-altered glass. Some varieties present a coarser grain size and sub-ophitic textures, suggesting a subvolcanic emplacement (Figure 8D). This unit is capped by massive conglomerate beds with 100% of the clasts of volcanic origin which, together with the volcanic lithologies, constitute an

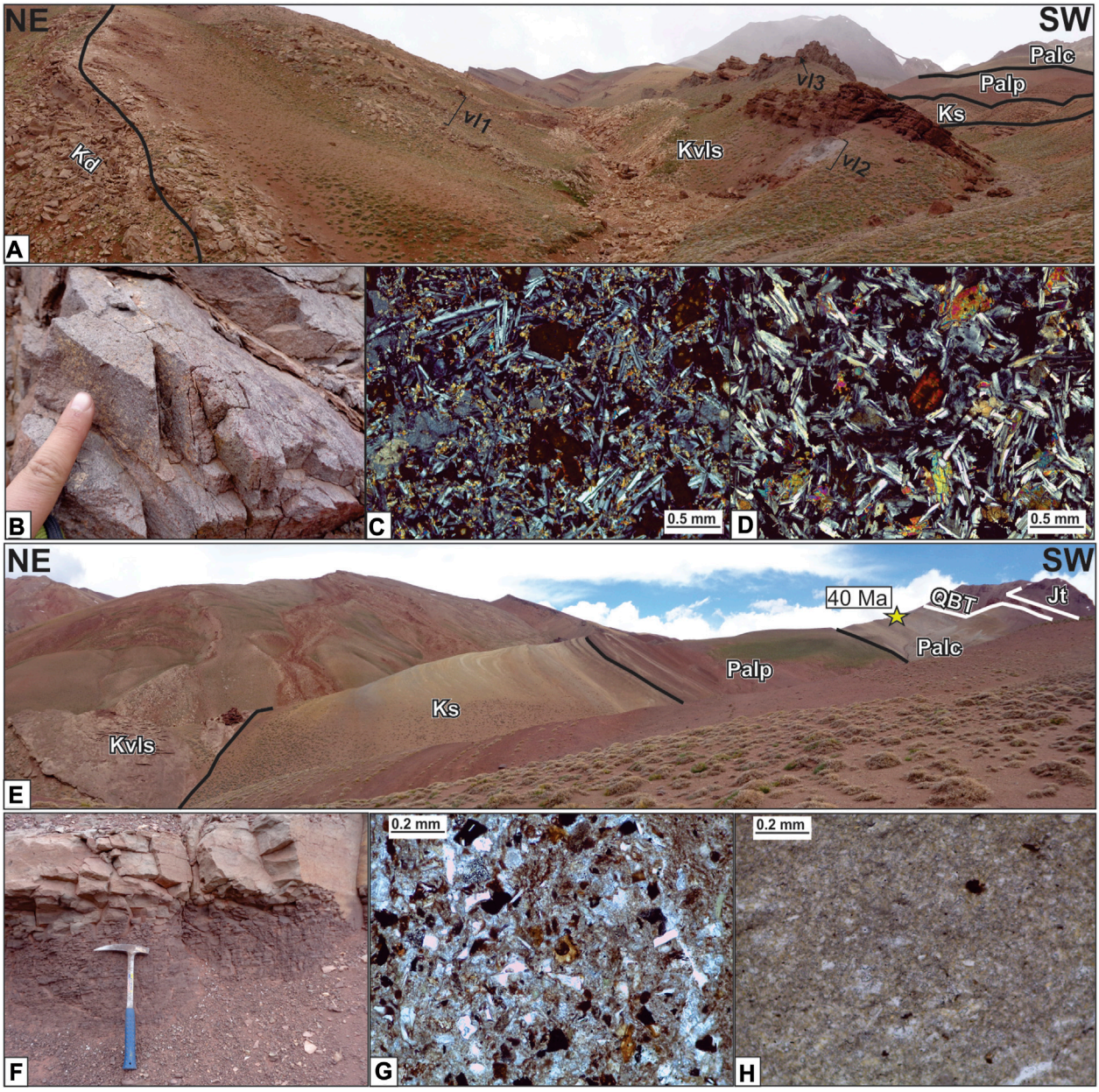

FIGURE 8
(A) The profile continues along a tributary of the Laguna Seca creek, where the contact between the Diamante Formation (Kd) and the Volcanitas Laguna Seca (Kvls) is evidenced with the appearance of mafic volcanic clasts in the conglomerates and three volcanic intercalations (vl1, vl2 and vl3). **(B)** Detail of the Volcanitas Laguna Seca volcanic rocks. **(C)** Under the microscope, these are porphyritic basalts characterized by olivine phenocrysts immerse within an intersertal groundmass. **(D)** Coarser-grained varieties of the basalts, where sub-ophitic textures are common with laths of plagioclase partially included in clinopyroxene crystals. **(E)** The Volcanitas Laguna Seca are followed by the Saldeño (Ks), Pircala (Palp) and Coihueco (Palc) formations, truncated at the top by the Quebrada Blanca thrust (QBT) that repeats the Tordillo Formation (Jt). **(F)** The Saldeño Formation consists of black shales and gray sandstones presenting reddish alterations. **(G)** At a microscopic scale, the calcareous sandstones of the Saldeño Formation show clasts of plagioclase and quartz with corroded borders. **(H)** The limestones of the Coihueco Formation correspond to micritic mudstones with a siliceous cement.

unequivocal evidence of its proximity to a volcanic center, possibly associated with the arrival of the Andean magmatic arc to the study area in latest Cretaceous times.

The sedimentary profile continues with a 5-m thick limestone, followed by 80 m of black shales intercalated with fine-grained calcareous sandstone beds (Figure 5) presenting red and yellow alterations, which we interpret as the latest Cretaceous Saldeño Formation (Figures 8E, F). An analysis under the petrographic microscope indicates that the calcareous sandstones are composed by clasts of plagioclase and quartz with embedded borders immersed in a carbonatic matrix and cemented by carbonate patches (Figure 8G) Although the age and depositional environment of this sequences must be studied in more detail, a complete analysis of this unit made by Tunik (2003) in the southern Aconcagua FTB suggests that its sedimentation took place, under the influence of the magmatic arc, during a maastrichtian Atlantic-derived marine

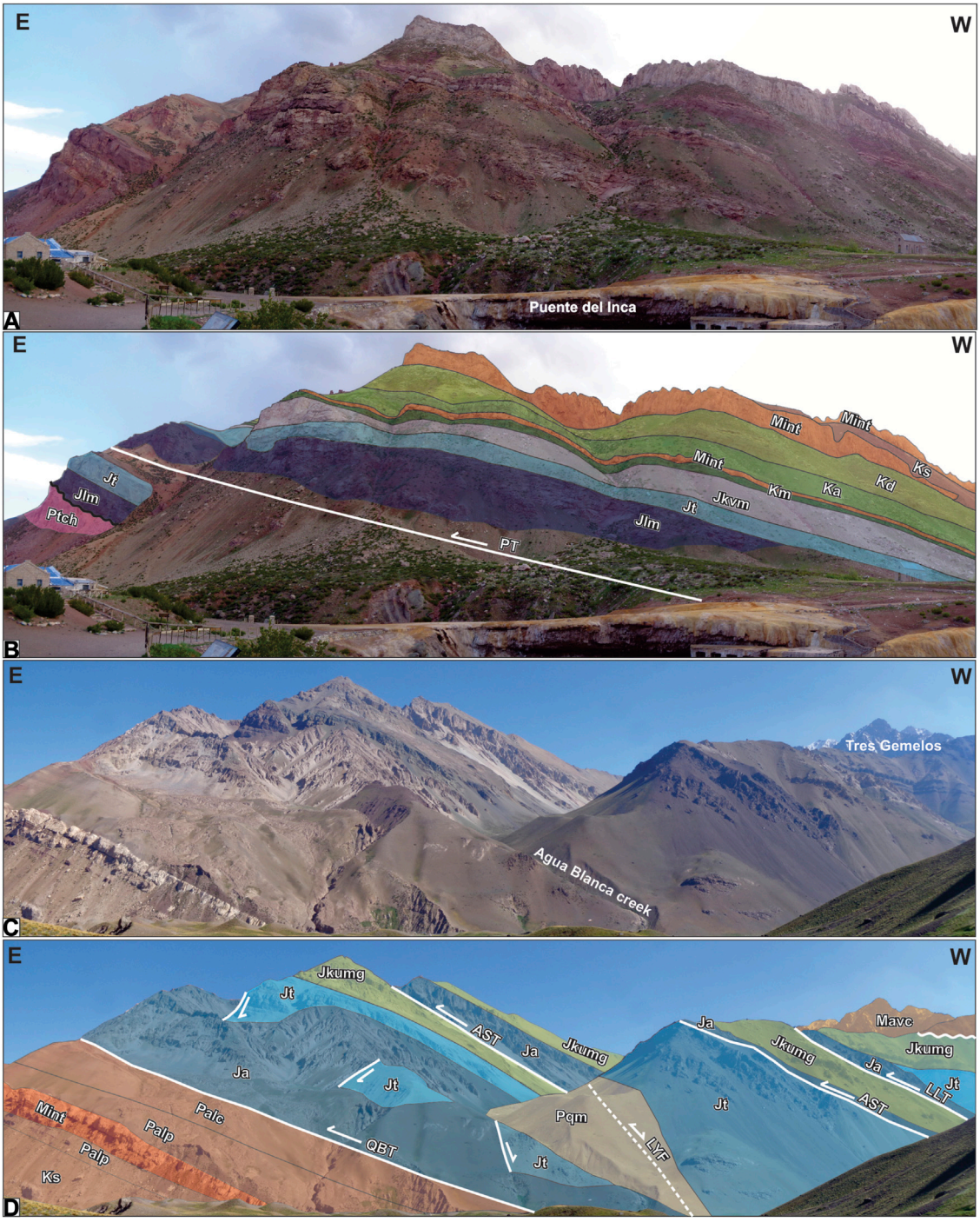

FIGURE 9
(A,B) Reinterpretation of the stratigraphy in the Puente del Inca classical locality, where white miocene trachytic sills (Mint) intrude the Cretaceous to Paleogene sequences (abbreviations of the different units and structures are the same as in Figure 7; Figure 8). **(C,D)** The Quebrada Blanca thrust detaches over gypsum deposits of the Auquilco Formation (Ja) transporting a series of undeformed half-grabens filled with the Tordillo Formation (Jt) and sealed by the marine deposits of the Upper Mendoza Group (Jkumg). The La Yesera fault (LYF), covered here by a Plio-Quaternary moraine (Pqm), corresponds to an inverted normal fault limiting an Upper Jurassic half-graben. A direct passage is observed between the Auquilco Formation and the Upper Mendoza Group in the hanging-wall of the Aguas Saladas thrust (AST), with no evidence of the Tordillo Formation. To the west, the Las Leñas Fault (LLF) exposes the Tordillo Formation again in its hanging-wall, where the deformed sequences of the Mendoza Group are unconformably overlain by the Aconcagua Volcanic Complex (Mavc).

transgression. This succession is followed by fine-grained massive red sandstones, which grade towards a 30 m-thick package of red claystones, and ends with 20 m of poorly-sorted massive volcaniclastic conglomerates (Figure 8E), which we assign to the Pircala Formation (Figure 5). This unit has also been detected in the southern Aconcagua FTB, but its study and temporal constraints to the

Paleocene-early Eocene are based on a series of works performed in the Malargüe FTB further south (Parras et al., 1998; Horton et al., 2016). The profile in the Laguna Seca creek ends with an alternation of shales and limestones, which under the microscope correspond to micritic mudstones with siliceous cement (Figure 8H). Although the paleoenvironment of these deposits must be resolved with future works, these facies are compatible with lacustrine sedimentation, and its stratigraphic position above the Pircala Formation makes them assignable to the Coihueco Formation (Figure 5). Despite not being described in the Aconcagua FTB before, these deposits have been recognized and dated by Horton et al. (2016) in the Malargüe FTB, where they obtained middle Eocene ages. The outcrops of the Coihueco Formation are interrupted by the Quebrada Blanca thrust, which repeats the Tordillo Formation (Figure 8E). These latest Cretaceous to Paleogene sequences have also been detected to the north in the Horcones River, to the south in the Blanco River and to the east in the Visera syncline (Figure 3).

3.3.3 Structural setting between Puente del Inca and Agua Blanca creek

The profile performed in the Vargas creek allowed us to reinterpret the stratigraphy exposed in the Puente del Inca, a classical locality of the Aconcagua FTB where the Penitentes thrust channels hot and mineralized waters to the surface, cementing quaternary detritus forming a natural bridge (Figure 9A, B). Three white volcanic sills known as the Puente del Inca trachytes are identified in this locality, intruding the Cretaceous to Paleogene sequences described in the previous section (Figure 3). These sequences constitute the foot-wall of the Quebrada Blanca thrust, whose characterization was performed through a complete survey of the Agua Blanca creek (Figure 3). A view of the eastern margin from the Cuevas River valley shows the gypsum deposits of the Auquilco Formation transporting a series of undeformed half-grabens filled with 200–300 m of the Tordillo Formation (Figure 9C, D). On the western margin of the creek, the Mesozoic deposits are deformed due to the activity of three different structures: La Yesera, Aguas Saladas and Las Leñas (Figure 3). While the La Yesera and Las Leñas faults had been identified previously, the Aguas Saladas thrust corresponds to a newly identified structure that presents a different stratigraphic arrangement in the hanging-wall, where the evaporites of the Auquilco Formation are directly covered by the marine deposits of the Upper Mendoza Group (Figure 9D). A sudden increase in thickness is observed in the outcrops of the Tordillo Formation exposed by the La Yesera fault, which we interpret as an inverted normal fault limiting an Upper Jurassic half-graben (Figure 9D). West of the Aguas Saladas thrust, the Tordillo Formation is exposed again by the Las Leñas fault, where the deformed Mesozoic sequences are unconformably overlain by the volcanic rocks of the Miocene Aconcagua Volcanic Complex (Figure 9D), previously mapped as part of the Juncal Formation (Figure 3).

3.3.4 Las Leñas, Navarro and El Fierro faults

The best place to observe the true nature of the Las Leñas fault is between the Agua Blanca creek and the Blanco River headwaters, where important N-S variations are observed in the thickness of the Tordillo Formation (Figure 3). West of the Aguas Saladas thrust, the Las Leñas fault exposes a red and grey sedimentary sequence, where a 440 m-thick sedimentary profile was performed and PGZ01 was sampled for U-Pb dating (Figure 10A). This sequence is composed by siltstones and sandstones in the lower section, siltstones and conglomerates with trough cross-bedding in the middle section (paleocurrents to the SE) and claystones interbedded with sandstones and conglomerates in the upper section (profile 3 in Figure 5). The sudden disappearance of these deposits both to the south and to the north can only be explained by the presence of an isolated depocenter filled by the Tordillo Formation and controlled by an Upper Jurassic normal fault (Figure 3). The inversion of this fault has exposed the half-graben at surface and generated an overturned frontal syncline in the Upper Mendoza Group deposits (Figure 10A). This area also has the best exposure of the 90° unconformable relation between the Upper Jurassic Tordillo Formation and the Miocene Aconcagua Volcanic Complex (Figure 10A).

The Cerro Negro, located between the Agua Blanca and Navarro creeks, represents another good place to observe the unconformable relation between the Tordillo Formation and the Miocene Aconcagua Volcanic Complex, main constitutent of the Cerro Tres Gemelos (Figure 3). The Tordillo Formation is exposed in the eastern margin of the Navarro creek as part of a long-wavelength syncline generated by the activity of the Navarro fault, which exposes, in the western margin, the temporal equivalent rocks of the Río Damas Formation (Figure 10B). An important thickness variation is observed between both Upper Jurassic units, indicating that the Navarro fault corresponds to a N-S trending inverted normal fault (Figure 10B). The thickness increase observed in the Upper Jurassic volcanic rocks had already been hinted by Sanguinetti and Cegarra (1991), who measured 900 m in this area and 1,200 m in the Cerro Tolosa to the north (Figure 3). The Río Damas Formation in this area is covered by the Upper Mendoza Group (Figure 10B), which is represented by shallow marine facies interbedded with volcanic deposits (Sanguinetti y Cegarra, 1991).

In the Cristo Redentor area, to the west, the Upper Mendoza Group deposits are covered by the red beds of the Cristo Redentor Formation, being both unconformably overlain by thick volcanic sequences previously mapped as the Juncal Formation, now assigned to the Abanico Formation (Figure 10C). One of the sedimentary profiles presented by Cristallini and Ramos (1996) from this area was inspected in order to understand the relations between the different units outcropping in this area (Figure 3). Although the contact between the Upper Mendoza Group and the Cristo Redentor Formation was not explored in detail, the inspection of the lower section showed it consists of claystones with intercalations of ostracode-rich limestones (profile 4 in Figure 5). A gypsum bed is observed interbedded with the claystones towards the top, which is separated by an important erosional boundary from a unit composed by volcanic breccias and volcanogenic deposits (Figure 5). The profile ends with a white tuff from where we obtained the sample CRT-1, which under the microcrope is characterized as a fine-grained vitric to crystalline tuff. This rock is formed by quartz, plagioclase and minor biotite crystal fragments, immersed in a groundmass formed by volcanic ash, devitrified to a fine-grained quartz-feldespatic assemblage, with spherulites and felisitic texture (Figure 10D). The age obtained from this tuff (CRT-1) allowed the reassignation of these deposits as part of the oldest terms of the Abanico Formation, and a reinterpretation of its basal contact with the Cristo Redentor Formation as unconformable instead of tectonic (Figure 10C). Both units together with their

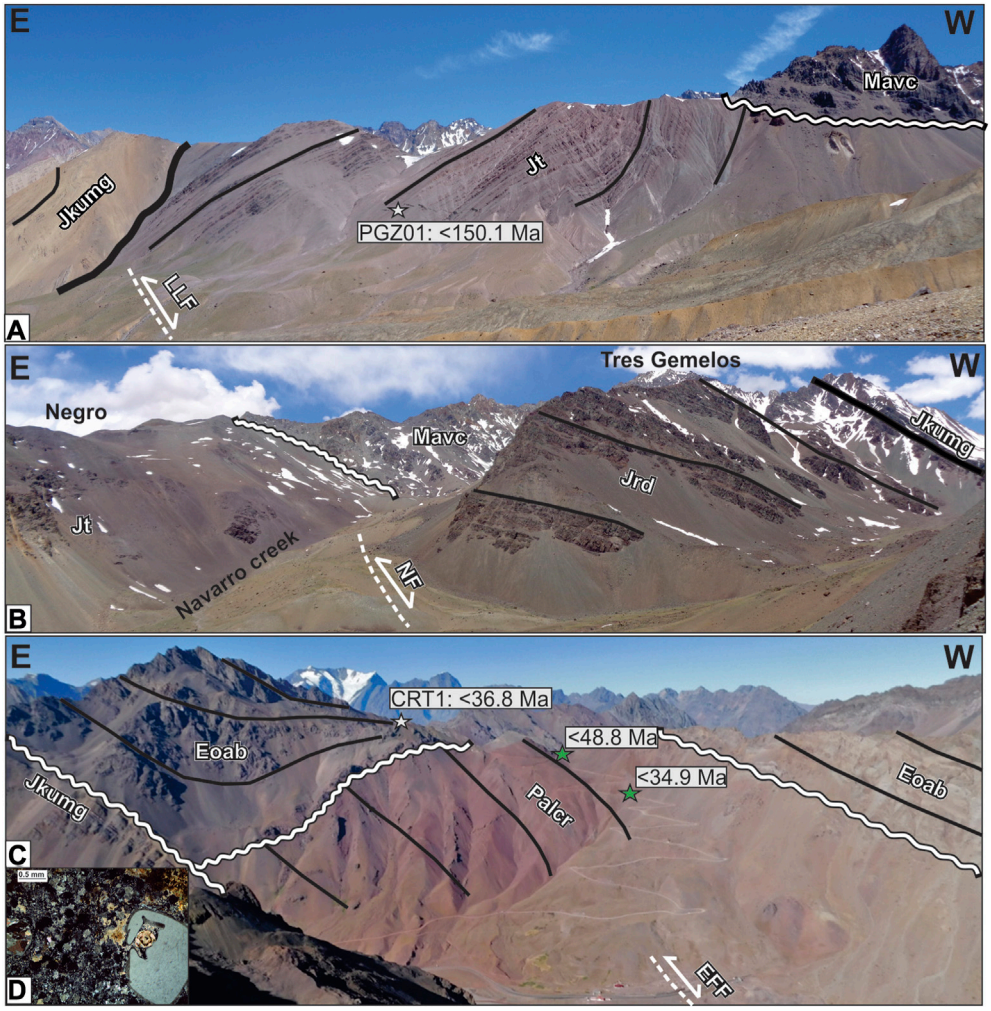

FIGURE 10
(A) The inversion of the Las Leñas Fault (LLF) in the Blanco River headwaters generated an overturned syncline in the Upper Mendoza Group (Jkumg) and exposed an Upper Jurassic half-graben filled by the Tordillo Formation (Jt), which is separated by an angular unconformity from the Miocene Aconcagua Volcanic Complex (Mavc). **(B)** The Navarro fault (NF) juxtaposes the Tordillo and Río Damas (Jrd) formations along the Navarro creek, where an important thickness increase to the west suggests it behaved initially as a normal fault, which is nowadays inverted. **(C)** The volcanic sequence overlying both the Upper Mendoza Group and Cristo Redentor Formation (Palcr) along the international border has been reinterpreted as the Abanico Formation (Eoab). Here, the activity of the El Fierro Fault (EFF) has generated a syncline and an anticline involving both the Cristo Redentor and Abanico formations. **(D)** Juvenile quartz, with embedded borders, within a fine-grained devitrified groundmass from the CRT1 dated tuff.

unconformable contact are folded generating a syncline and an anticline that can be observed in the Cristo Redentor area (Figure 10C), which we interpret as generated by the activity at depth of the N-S trending El Fierro Fault (Figure 3), an inverted normal fault interpreted as the eastern border of the Abanico basin (Charrier et al., 2002; Farias et al., 2010; Piquer et al., 2015).

4 Discussion

4.1 Temporal constraints for the timing of deformation in the Aconcagua FTB

With the great amount of geochronological data available and all the new structural, geological and sedimentological observations, the timing of deformational events in the Aconcagua FTB appears to be more complex that previously thought. Therefore, in order to discuss the different stages, we divided the Aconcagua FTB into three structural domains: inner, middle and frontal; each with a particular style and timing of deformation. Due to its clear and emblematic exposures, the northern margin of the Cuevas River will be used to describe the deformational timing of each of this sectors.

4.1.1 The inner structural domain

Two major reverse faults are responsible for the structuration of the inner domain: the Navarro and El Fierro faults (Figure 3). The Navarro fault would have behaved as a normal fault during the Late Jurassic, as indicated by the changes of thickness recorded between the nonmarine deposits of Tordillo Formation and the volcanic and volcaniclastic deposits of the Río Damas Formation. The initial stages of inversion of this fault must have taken place after the Lower Cretaceous and before the Paleocene, given the unconformable

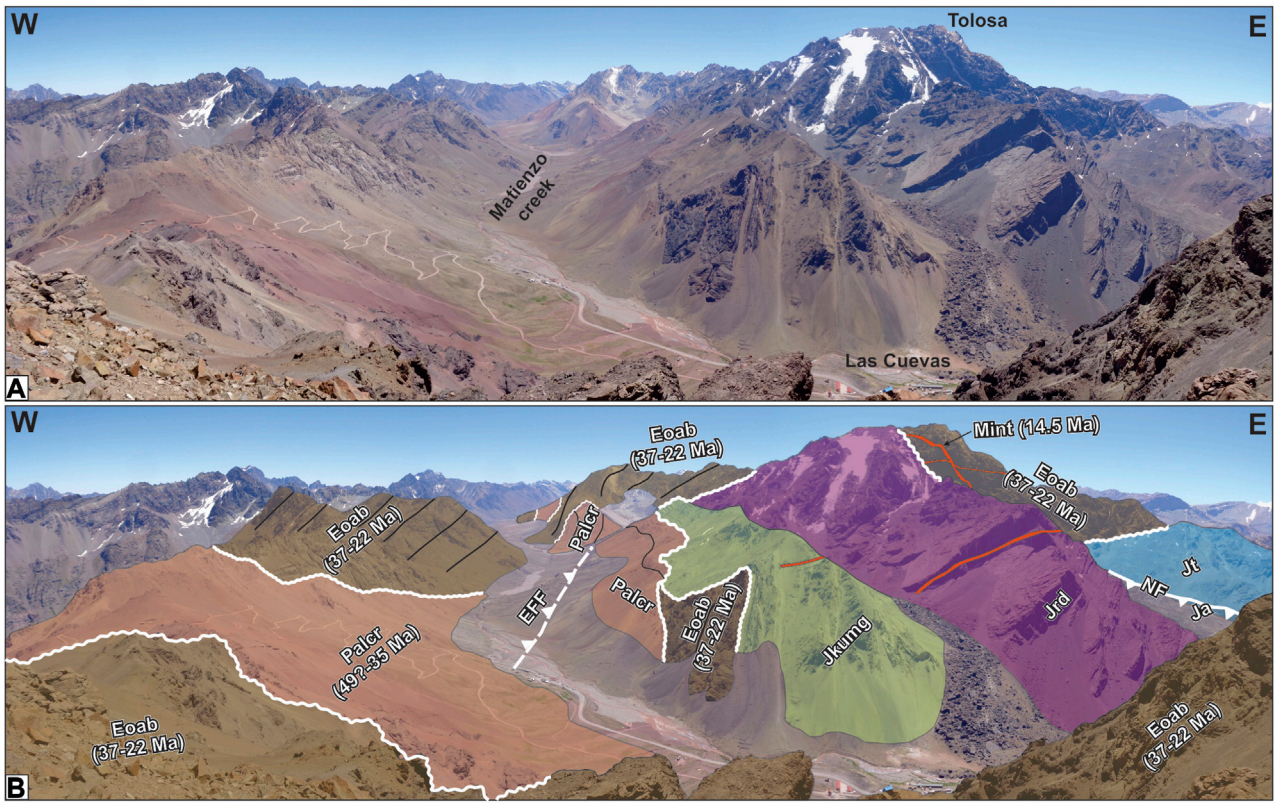

FIGURE 11
(A) View of the inner structural domain along the northern margin of the Cuevas River. **(B)** The cross-cutting relations observed in the inner structural domain suggest it was deformed in at least three stages: Late Cretaceous, Paleocene-Middle Eocene and early Miocene. Abbreviations are the same as in previous figures.

relation and existing hiatus between the Upper Jurassic-Lower Cretaceous Mendoza Group deposits and the Cristo Redentor and Abanico formations (Figure 11). Although the oldest temporal constraint available for the Cristo Redentor Formation in the study area is a maximum depositional age of 48.8 Ma, a Paleocene maximum depositional age of 60.9 Ma was obtained from its basal section in the La Ramada FTB to the north (Mackaman-Lofland et al., 2019). Therefore, despite different interpretations regarding the duration of the hiatus in this area, the most probable age for the reverse reactivation of the Navarro fault is the Late Cretaceous. This event would have been contemporary with the deposition of the Diamante Formation, which crops out towards the east, in the middle and frontal domains (Figure 3). The Diamante Formation has been interpreted in several works as the first synorogenic deposits of the Andean foreland basin (Gómez et al., 2019; Mackaman-Lofland et al., 2019; Martos et al., 2020). The erosive unconformity between the Agrio and Diamante formations brackets a hiatus of at least 30–25 Ma, which had already been identified in the Malargüe FTB associated with a Late Cretaceous contractional stage (Balgord and Carrapa, 2016; Fennell et al., 2017; Borghi et al., 2019). Moreover, the presence of limestone clasts in the conglomerates of the Diamante Formation and Middle Jurassic to Lower Cretaceous detrital zircons in sandstones sampled from this unit (Figure 6) suggest erosion of the underlying deposits during deposition. On the other hand, the presence of rhyolites and quartz in the conglomeratic clastic population, and the important Gondwanic peaks (*ca.* 254 and 278 Ma) exhibited in both U-Pb detrital zircon patterns (Figure 6) algo suggest that outcrops of the Choiyoi Group were exposed during this stage. These evidences support the interpretation of Martos et al. (2020), which proposes that the Frontal Cordillera, to the east, acted as a topographic high during Late Cretaceous times.

The following deformational stage is constrained by the angular unconformity between the Cristo Redentor and Abanico formations (Figure 10; Figure 11), a relation that had already been described by Aguirre Le Bert (1960) and confirmed by Yrigoyen (1979). However, our new field observations suggest that, to the west, the angularity disappears, and the passage between the Cristo Redentor and Abanico formations is transitional, which agrees with the similar ages obtained for both formations (Figure 10; Figure 11). Based on the maximum depositional ages available, deformation must have taken place between Paleocene and middle Eocene times, of which there are several lines of evidence close to the study area (Charrier et al., 2015; Lossada et al., 2020b). Further work must be done in order to understand the true impact of this stage in the study area, in particular, targeting the recently recognized deposits of the Pircala Formation deposited during this event.

The El Fierro Fault acted as a basin-bounding normal fault during deposition of the Abanico Formation, whose available ages indicate that occurred between 37 and 22 Ma (Figure 11) (Piquer

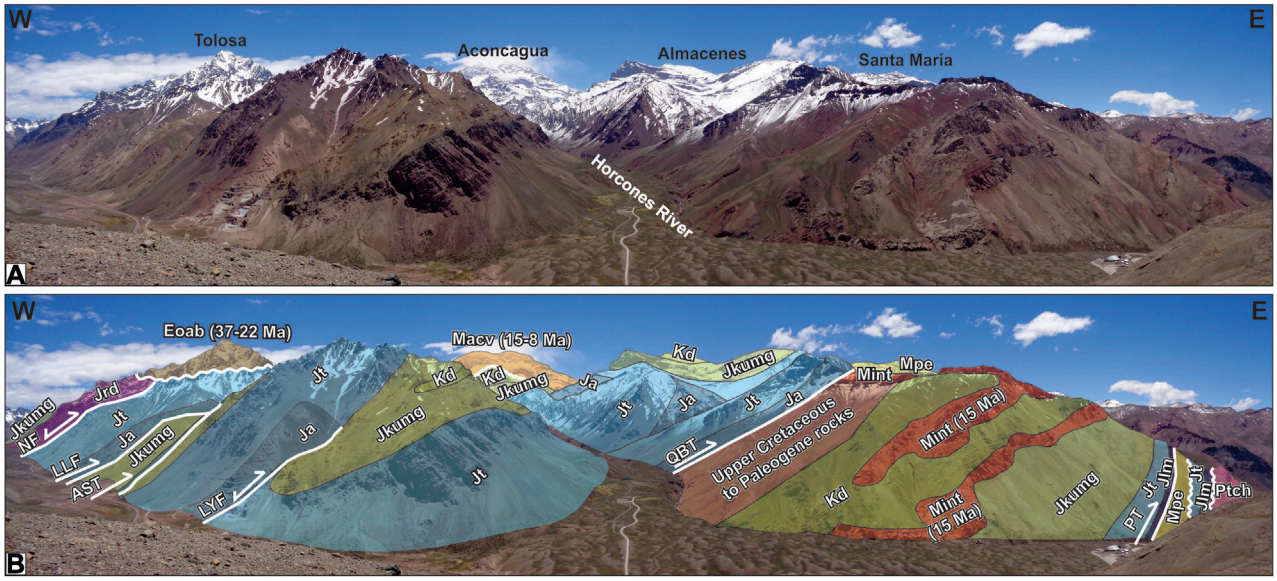

FIGURE 12
(A) View of the middle structural domain along the northern margin of the Cuevas River. **(B)** The unconformity at the base of the syncline filled with the Abanico Formation in the Cerro Tolosa, the angular unconformity at the base of the Aconcagua Volcanic Complex in the Cerro Aconcagua and the undeformed Miocene white trachytic intrusions suggest that the middle structural domain was deformed in at least two stages: the first during the early Paleogene and the second in the early Neogene. Abbreviations are the same as in previous figures.

et al., 2015). Since the outcrops of the Abanico Formation appear deformed in the inner domain, the inversion of the El Fierro Fault must have taken place after the Oligocene (Figure 11). An upper temporal constraint for this event is given by the presence of undeformed Miocene white trachytes dated in 14.5 Ma in the Cerro Tolosa area by Ramos et al. (1996b), which are intruding a syncline filled with volcanic deposits, interpreted as outcrops of the Abanico Formation based on our new data (Figure 11). Therefore, the best constraint available for this last stage is between 22 and 14.5 Ma, in agreement with the age estimated for the angular unconformity between the Abanico and Farellones formations in Chile (Charrier et al., 2002; Fock et al., 2006; Armijo et al., 2010; Piquer et al., 2015; Riesner et al., 2018).

4.1.2 The middle structural domain

The middle structural domain comprises 4 different structures with similar characteristics: Las Leñas, Aguas Saladas, La Yesera and Quebrada Blanca (Figure 3). In this domain, the temporal constraints for the deformational stages are given by the potential Paleogene depositional age of the newly recognized deposits in the foot-wall of the Quebrada Blanca thrust, and the available ages of the Abanico Formation and Aconcagua Volcanic Complex deposits, which can be seen covering unconformably the Las Leñas and Quebrada Blanca reverse fault sheets, respectively (Figure 12). Since the oldest date of the Abanico Formation in the study area is the crystallization age of 36.82 ± 0.37 Ma presented in this work, deformation must have taken place before, during early Paleogene times, but after deposition of the Diamante Formation, which can be observed in a tight overturned syncline in the western margin of the Horcones river (Figure 3; Figure 12). However, the Abanico Formation is deformed generating a syncline, suggesting movement of the Las Leñas fault after deposition (Figure 12). Therefore, since the outcrops of the Aconcagua Volcanic Complex are nearly horizontal in this domain, deformation must have ended before 15 Ma (Ramos et al., 1996b), also confirmed by the undeformed Puente del Inca white trachytic intrusions along this domain (Figure 12).

4.1.3 The frontal structural domain

A couple of thrusts characterize the frontal structural domain: Penitentes and Santa Maria (Figure 3). While the activity of the Penitentes thrust must have began, if our interpretations are correct, after deposition of the Coihueco Formation (40 Ma), it should have occurred before 15–12 Ma, given the available ages for the Penitentes conglomerates located in the foot-wall (Figure 3; Figure 13) (Carrapa et al., 2022; Martos et al., 2022). This is also confirmed by the age of the rather undeformed Puente del Inca trachytes (15 Ma) intruded along the thrust sheet (Ramos et al., 1996b). On the other hand, the activity in the Santa Maria thrust must have began at least <8 Ma, given the youngest available ages for the Santa Maria Volcanic Agglomerates, which appear on the foot-wall of this thrust (Figure 13) (Vicente, 2005). Since no plio-quaternary deformation has been documented in this area, deformation must have ceased in late Miocene times, coeval with the shutdown of the magmatic arc (Ramos et al., 2002).

4.2 Upper Jurassic extensional architecture

During the past two decades, the Late Jurassic has been reinterpreted as a stage of extensional deformation in the Aconcagua region (Giambiagi et al., 2003a; Vicente and Leanza, 2009; Acevedo et al., 2020; Mardones et al., 2021), in line with what is being described in other nearby sectors (Mescua et al., 2008;

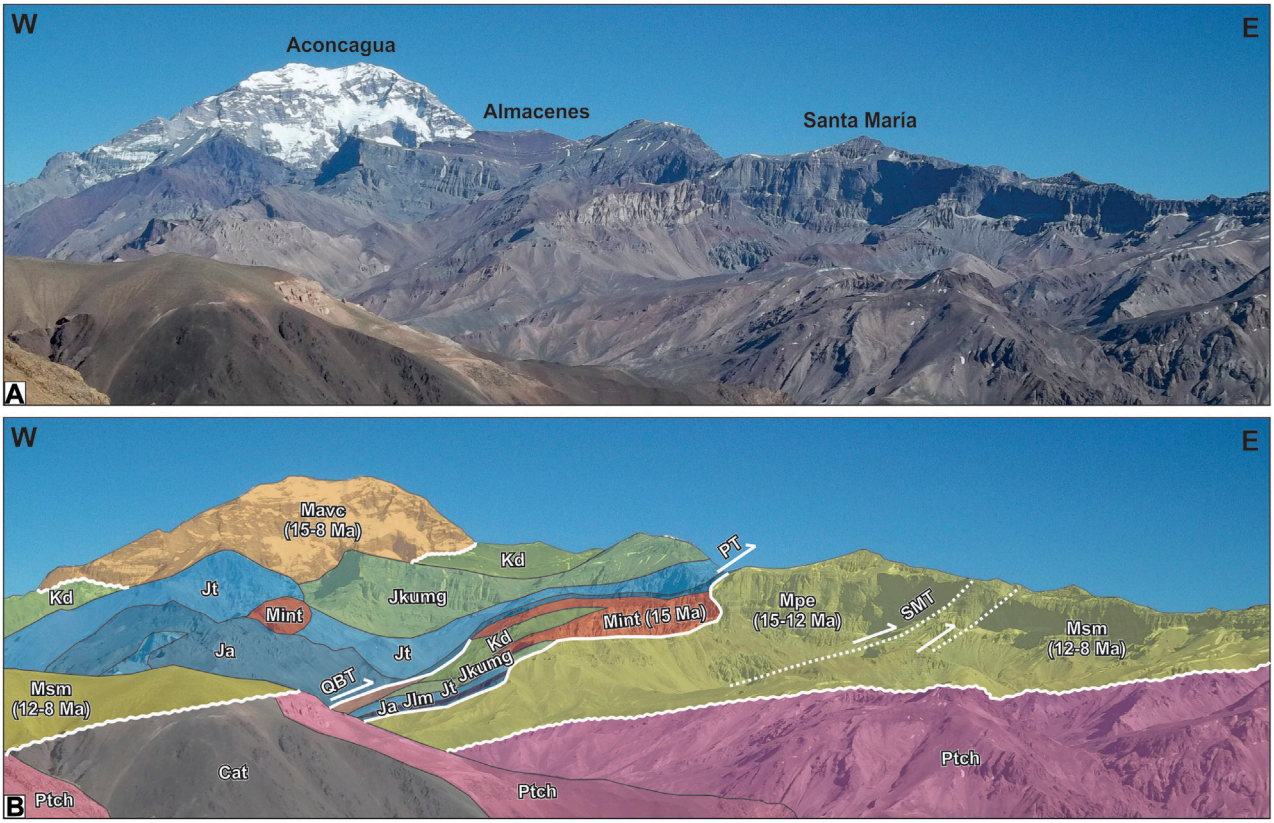

FIGURE 13
(A) View of the frontal structural domain along the northern margin of the Cuevas River. **(B)** The frontal structural domain was shortened during the Neogene, given the available ages of the Penitentes Conglomerates in the foot-wall of the Penitentes thrust, and of the Puente del Inca trachytes intruding the thrust plane. A minor thrusting event must have taken place after deposition of the Santa Maria Volcanic Agglomerates, which constitute the foot-wall of the Santa Maria thrust. Abbreviations are the same as in previous figures.

Martos et al., 2020; Acevedo et al., 2022). In this sense, the new observations presented in this work combined with the various sedimentological profiles available for the Tordillo and Río Damas formations in the area, allowed the reconstruction of the Upper Jurassic extensional architecture along the Cuevas river section (Figure 14).

Several half-grabens have been observed from west to east, which can be divided into three sectors, each of them separated by structural highs interpreted as horsts: the western, middle, and eastern sectors (Figure 14). The western sector contains 1,200 m of volcanic rocks and coarse alluvial deposits (Las Cuevas profile, Sanguinetti and Cegarra, 1991) and at least 440 m of fine-grained fluvial deposits (Las Leñas profile, this work). To the east, the Upper Mendoza Group marine deposits directly overlay the evaporites of the Auquilco Formation (Aguas Saladas profile), defining a horst that divides the western and middle sectors. The middle sector shows thickness variations between 600 and 200 m from west to east and is dominated by fluvial conglomerates and sandstones (Horcones profile, Cegarra, 1994; Blanco River II; Acevedo et al., 2020). To the east, the Vargas profile contains only 9 m of conglomerates attributed to the Tordillo Formation, overlying the La Manga Formation limestones, since the Auquilco Formation is absent, defining another horst that divides the middle and eastern sectors. The eastern sector presents fluvial conglomerates and sandstones between 60 and 20 m from west to east (Puente del Inca, Lo Forte, 1996; Blanco River I, Acevedo et al., 2020).

Thickness variations combined with field observations helped define the major normal faults that were active during deposition of the Upper Jurassic Tordillo and Río Damas formations. In the western sector, the Las Cuevas and Las Leñas depocenters would be controlled by the Navarro and Las Leñas faults, respectively (Figures 10A, B). The Aguas Saladas thrust (Figure 9D) exposes the Upper Mendoza Group directly overlaying the Auquilco Formation, which shows the absence of the Tordillo Formation and defines a horst. In the middle sector, the La Yesera fault (Figure 12) would have controlled the Horcones depocenter, while the Quebrada Blanca thrust exposes non-inverted half-grabens (Figure 9D) that could be linked to the Blanco River II depocenter. At Vargas Creek (Figure 7B), the absence of the evaporites of the Auquilco Formation and the thin beds of the Tordillo Formation (9 m) suggest the presence of another structural high. Finally, the eastern sector, although less developed, also presents non-inverted half-grabens (Figure 7A).

The provenance and paleogeography of the area were previously studied by Lo Forte (1996), who suggested two source areas, a western contemporaneous source, the volcanism of the Río Damas Formation, and an eastern source, the Permo-Triassic Choiyoi Group. For the middle sector, Lo Forte (1996) proposed the

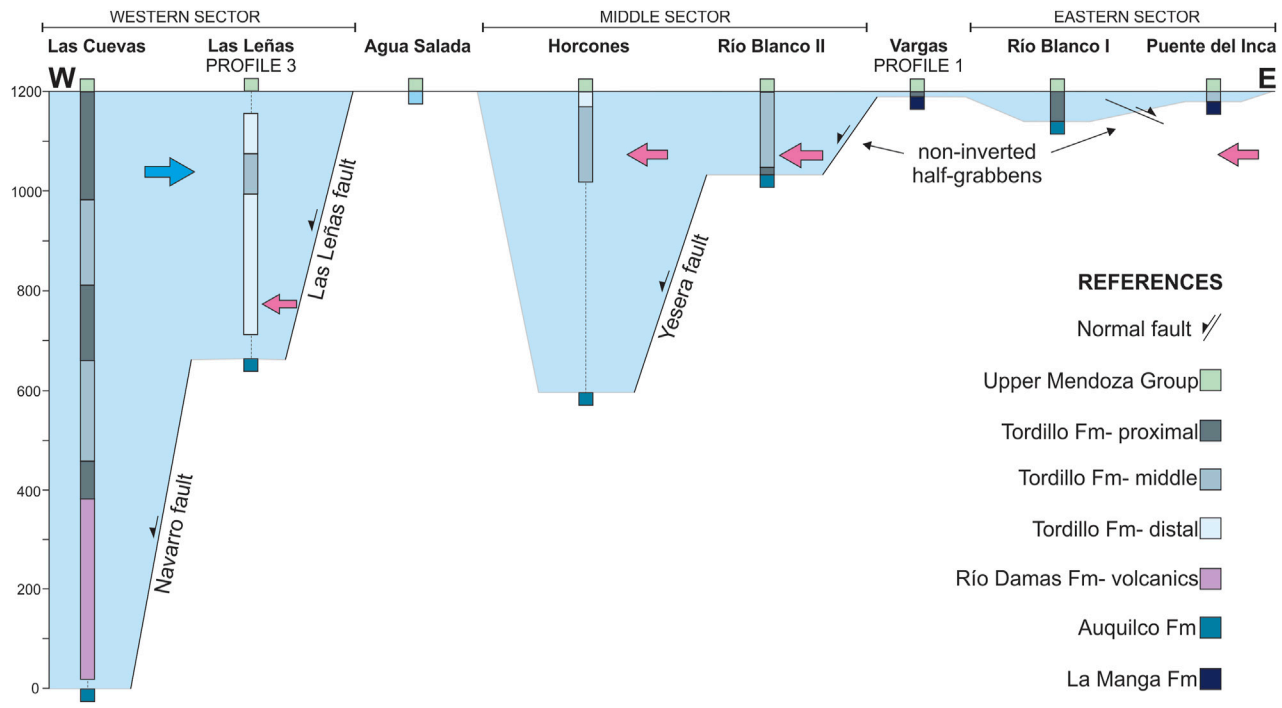

FIGURE 14
Schematic stratigraphic transect showing the W-E distribution of the Tordillo and Río Damas formations between the Cuevas and Blanco rivers. Las Cuevas section was measured by Sanguinetti and Cegarra (1991); Horcones section by Cegarra (1994); Blanco River I and II by Acevedo et al. (2020); Puente del Inca by Lo Forte (1996); Las Leñas, Vargas and Aguas Saladas are based on this work. While the blue arrow indicates provenance from the contemporaneous magmatic arc represented in the Río Damas Formation, the pink arrow shows provenance from the eastern basin margin, dominated by outcrops of the Choiyoi Group nowadays exposed in the Frontal Cordillera.

existence of an endorheic playa-lake that drained both fluvial systems. These interpretations, combined with the new structural and geochronological evidence presented, allows to reconstruct a more complex paleogeography. The western sector presents a proximal to distal facies distribution from west to east (Figure 14) and, although the expected main source is the volcanism of the Río Damas Formation, the sample PGZ01 (Las Leñas, profile 3; Figure 5) shows a multimodal pattern of U-Pb detrital zircon ages (Figure 6). The sample has main peaks of Gondwanan and pre-Andean ages that may agree with a scenario of rifting and exposure of the underlying units (pre-Andean) and the basement (Gondwanian). Contemporaneous ages are also present, suggesting the Rio Damas magmatism was also a source. Towards the top of Profile 3 (Las Leñas), coarser fluvial facies appear and paleocurrent measurements show an eastward flow direction (Figure 5). This change may indicate rerouting of sediment and the prevalence of the Río Damas magmatism as the main source. Petrographic descriptions of sandstone samples from the middle and eastern sectors show a predominance of acid volcanic clasts, which are attributed to the eastern Permo-Triassic Choiyoi Group (Cegarra, 1994; Lo Forte, 1996). Also, the presence of limestone clasts in the Blanco River II profile suggests exposure and erosion of the underlying La Manga Formation (Acevedo et al., 2020).

In this scenario, the basin during the sedimentation of the Upper Jurassic Tordillo and Río Damas formations would have been segmented due to rifting, with two distinct depocenters in the Aconcagua region (Figure 14). The western depocenter shows higher thickness values and interbedded volcanism, while the eastern depocenter would have been thinner and strictly clastic. While both depocenters' provenance would be conditioned by local rifting and exposure of the underlying units, the western depocenter would have the Río Damas magmatism as its main source and the eastern depocenter would be mainly sourced from the Permo-Triassic Choiyoi Group.

4.3 Tectonic evolution of the Aconcagua FTB and implications for Andean-mountain building models

In order to condense all the interpratations based on the new data and previous works and propose a tectonic evolution for the Aconcagua FTB, we built a schematic cross-section along the Cuevas River (Figure 15A). It should be noted that the structural setting at depth is based solely on our interpretations of the surface geology, which leaves the modeling assessing its feasibility for a future project. Nevertheless, the presence of important seismicity at a depth of 10–15 km beneath the Aconcagua FTB between 33° and 34°S could suggest the presence of a detachment located in the pre-Jurassic basement, deeper than previously thought for this area (Olivar et al., 2018; Ammirati et al., 2019).

One of the main new interpretations is that the inversion of normal faults is a key mechanism behind the present structure of the Aconcagua FTB, as evidenced along the three different structural domains defined in this work. In the inner domain, a thick-skinned

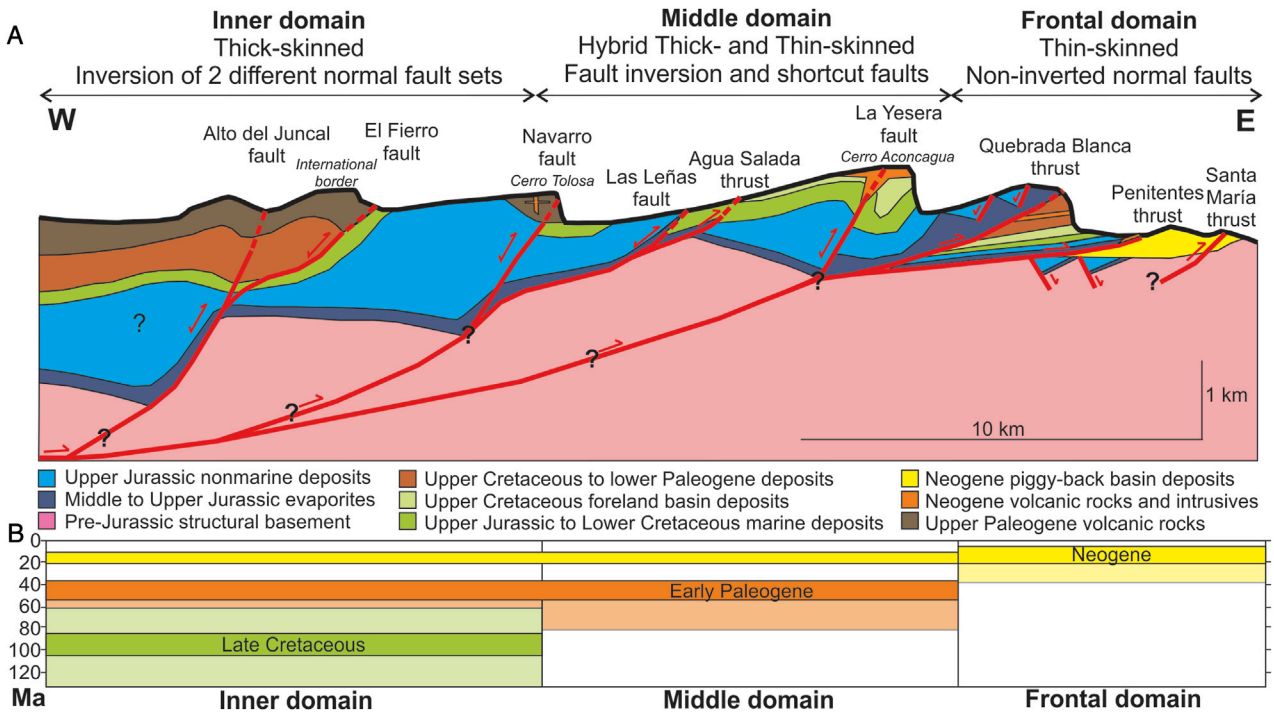

FIGURE 15
(A) Schematic representation of the Aconcagua FTB based on our interpretation of the new data obtained in this work. It should be noted that reverse faults represented at surface by dashed red lines can be found in the study area either cutting topography, in subsurface (blind), or covered by younger volcanic units. However, while the structure at depth is speculative, future models should include the inversion of normal faults as a new mechanism in this belt. **(B)** Our preferred interpretation regarding activity of the reverse faults in each domain suggests an advancing deformational front that expanded eastwards in at least three discrete pulses: Late Cretaceous, Middle Eocene and Miocene. The temporal constraints (transparent boxes) for each pulse are the following: Inner domain, 130–60.9 Ma/60.9–37 Ma/22–14.5 Ma; Middle domain, 80–37 Ma/22–15 Ma; Frontal domain, 40–15 Ma/12–5 Ma (see text for details).

deformational style was interpreted due to tectonic inversion of the Navarro and El Fierro normal faults, exposing both Late Jurassic and late Eocene to early Miocene half-grabens at surface, respectively (Figure 15A). The El Fierro fault has been interpreted as linked at depth with the Alto del Juncal fault in Chile (Piquer et al., 2015), being afterwards inverted as a shortcut fault (Figure 15A) (Piquer et al., 2015). On the other hand, the presence of 420 m of conglomerates, sandstones and limestones below gypsum deposits attributable to the Auquilco Formation south of the Navarro creek (Aguirre Le Bert, 1960), suggests a deeper detachment for the Navarro fault, probably rooted into the basement (Figure 15A). At least three contractional stages were detected in this domain, which occurred in the Late Cretaceous, the early Paleogene and the early Neogene (Figure 15B). To the east, in the middle domain, a hybrid thick- and thin-deformational style is observed, where the inversion of normal faults, the Las Leñas and La Yesera, has produced a series of shortcut faults, the Aguas Saladas and Quebrada Blanca thrusts, through their insertion into the sedimentary cover (Figure 15A). Despite not exposing any units below the Auquilco Formation, we interpret that the Las Leñas fault is rooted into the Navarro fault, and that the La Yesera fault could be cutting directly into the pre-Jurassic structural basement (Figure 15A). Deformation in this domain took place in at least two events, which we locate in the early Paleogene and in the early Neogene (Figure 15B). Finally, the frontal domain is dominated by the presence of non-inverted Late Jurassic normal faults transported or bypassed by the thin-skinned Penitentes and Santa Maria thrusts (Figure 15A), whose activity occurred in two stages: early and late Neogene (Figure 15B).

Taken all together, the changes in structural style and deformational timing between the different domains would indicate a shallowing of the detachment in the Aconcagua FTB as the deformational front advanced towards the east, a process that appears to have been occurring since Late Cretaceous times. This would suggest that while thick-skinned mechanisms likely occurred during the older stages, late Cretaceous and early Paleogene, thin-skinned deformation took place after tectonic inversion, probably as shortcut faults and new thrusts during the Neogene (Figure 15). This interpretation falls in line with the hypothesis developed by Mouthereau et al. (2013), who proposed that inherited lithospheric strength influences deformational style during contraction. Late Jurassic rifting thinned the lithosphere in the Aconcagua region, resulting in weak mechanical coupling with the crust, which favored thick-skinned structures during the beginning of contraction. This initial stage would have occurred in Late Cretaceous times, in agreement with what has been proposed both to the north and to the south of the study area (e.g., Borghi et al., 2019; Mackaman-Lofland et al., 2019).

5 Conclusion

A complete revisit of the classical Cuevas River section has been performed during this work, which included a thorough bibliographic review, a series of new and original geological and structural observations, the logging of 4 sedimentary profiles and the U-Pb zircon dating of 4 samples taken from different units in key areas. The stratigraphic column and geological map of the Aconcagua region in the Cuevas river section have been updated, which include a complete rearrangement of the red beds and volcanic units and the recognition of a latest Cretaceous to Paleogene record not previously described in this area. This update also included a complete characterization of the Tordillo Formation along the Cuevas River section, evidencing its deposition during a Late Jurassic extensional event. The structural style of the Aconcagua FTB has been shown to be the result of the tectonic inversion of the Late Jurassic extensional architecture, which is nowadays reflected by a combination of thick-skinned, hybrid and thin-skinned mechanisms. The timing of deformation has been improved, showing a polyphasic history beginning in the Late Cretaceous in the inner thick-skinned structural domain, advancing into the middle hybrid domain during the Paleogene, and reaching the thin-skinned frontal domain in the Neogene. This type of progression of the orogenic front not only suggests a shallowing of the decollement and an east-vergent mode of deformation, but also highlights the Late Cretaceous as the initial deformation stage at these latitudes, which should be considered in future Andean mountain-building models.

Data availability statement

The original contributions presented in the study are included in the article/Supplementary Material, further inquiries can be directed to the corresponding author.

Author contributions

LMF, FEM, NAP, EA, LFP, LM, MS, MN, and AF contributed to the conception, design and data acquisition of the study. NH was in charge of U-PB zircon dating. LFP, LM, and VL performed the petrographic analyses of thin sections. LMF wrote the first draft of the manuscript. FEM and EA wrote a section of the manuscript. LMF, FEM, and EA made the figures. AF, MN, and VL supervised and provided funding for the project. All authors contributed to the article and approved the submitted version.

Funding

This study has been funded by the grants PICT-2019-974, PICT-2019-2558, PIP 11220200102730CO and UBACYT 20020190100234BA.

Acknowledgments

We would like to acknowledge Daniel Perez and Victor Ramos for counsel about the geology and access to the study area, Beatriz Aguirre-Urreta and Martin Hoqui for fossil identification in the Mesozoic marine units and Eduardo Rosselot, Sofía Iannelli, Maximiliano Perez Frasette, Lucrecia Cavallero and Emiliano Cristiano for their assistance in the field. Help from the Escuadrón N° 27 of Gendarmeria Nacional in Punta de Vacas is deeply appreciated. We are grateful with the editor LG, Frederic Mouthereau and Cesar Witt for their comments and suggestions, which greatly improved the manuscript. We hope this work constitutes an inspiration to the new generations of geologists, driving them to the field to visit both highly explored and unexplored areas. We would like to dedicate this work to the memory of Jean-Claude Vicente, a great Andean geologist whose work constitutes a pillar in the knowledge of this region. This is the R-467 contribution of the Instituto de Estudios Andinos Don Pablo Groeber (IDEAN, UBA-CONICET).

Conflict of interest

The authors declare that the research was conducted in the absence of any commercial or financial relationships that could be construed as a potential conflict of interest.

Publisher's note

Supplementary material

The Supplementary Material for this article can be found online at: https://www.frontiersin.org/articles/10.3389/feart.2023.1219351/full#supplementary-material

References

Acevedo, E., Fernández Paz, L., Encinas, A., Horton, B. K., Hernando, A., Valencia, V., et al. (2022). Late jurassic back-arc extensión in the neuquén basin (37°S): insights from structural, sedimentological and provenance analyses. *Basin Res.* 35, 1012–1036. doi:10.1111/bre.12744

Acevedo, E., Rosselot, E. A., Martos, F., Fennell, L., Naipauer, M., and Folguera, A. (2020). "Tectonic setting of the Tordillo Formation in the Aconcagua fold-and-Thrust belt," in *Opening and closure of the neuquén basin in the southern Andes*. Editors D. Kietzmann, and A. Folguera (Springer Earth System Sciences), 159–174.

Aguirre Le Bert, L. (1960). *Geología de los Andes de Chile Central: Provincia de Aconcagua Publicaciones del Instituto de Investigaciones Geológicas*, 9. Santiago de Chile: Editorial Universitaria.

Aguirre-Urreta, M. B., and Lo Forte, G. L. (1996). "Los depósitos tithoneocomianos," in *Geología de la región del Aconcagua, provincias de San Juan y Mendoza*. Editors V. A. Ramos, M. B. Aguirre-Urreta, P. P. Álvarez, M. I. Cegarra, E. O. Cristallini, S. M. Kay, et al. (Buenos Aires: Anales de la Dirección Nacional del Servicio Geológico, Subsecretaría de Minería de la Nación), 179–229.

Aguirre-Urreta, M. B., and Ramos, V. A. (1996a). "Reseña de la exploración geológica," in *Geología de la región del Aconcagua, provincias de San Juan y Mendoza*. Editors V. A. Ramos, M. B. Aguirre-Urreta, P. P. Álvarez, M. I. Cegarra, E. O. Cristallini, S. M. Kay, et al. (Buenos Aires: Anales de la Dirección Nacional del Servicio Geológico, Subsecretaría de Minería de la Nación), 9–15.

Allmendinger, R. W., Figueroa, D., Snyder, D., Beer, J., Mpodozis, C. M., and Isacks, B. L. (1990). Foreland shortening and crustal balancing in the Andes at 30°S Latitude. *Tectonics* 9 (4), 789–809. doi:10.1029/tc009i004p00789

Ammirati, J. B., Vargas, G., Rebolledo, S., Abrahami, R., Potin, B., Leyton, F., et al. (2019). The crustal seismicity of the western andean thrust (Central Chile, 33°-34°S): implications for regional tectonics and seismic hazard in the santiago area. *Bull. Seismol. Soc. Am.* 19 (5), 1985–1999. doi:10.1785/0120190082

Armijo, R., Rauld, R., Thiele, R., Vargas, G., Campos, J., Lacassin, R., et al. (2010). The West andean thrust, the san ramón fault, and the seismic hazard for santiago, Chile. *Tectonics* 29, TC2007. doi:10.1029/2008TC002427

Balgord, E. A., and Carrapa, B. (2016). Basin evolution of upper cretaceous-lower cenozoic strata in the Malargüe fold-and-thrust belt: northern neuquén basin, argentina. *Basin Res.* 28, 183–206. doi:10.1111/bre.12106

Borghi, P., Fennell, L., Gómez Omil, R., Naipauer, M., Acevedo, E., and Folguera, A. (2019). The neuquén Group: the reconstruction of a late cretaceous foreland basin in the southern central andes (35-37°s). *Tectonophysics* 767, 228177. doi:10.1016/j.tecto.2019.228177

Bressan, G. S., and Palma, R. (2010). Taphonomic analysis of fossil concentrations from La Manga Formation (oxfordian), neuquén basin, Mendoza province, Argentina. *J. Iber. Geol.* 36 (1), 55–71. http://revistas.ucm.es/index.php/JIGE/article/view/JIGE1010120055A.

Buelow, E. K., Suriano, J., Mahoney, J. B., Kimbrough, D. L., Mescua, J. F., Giambiagi, L. B., et al. (2018). Sedimentologic and stratigraphic evolution of the Cacheuta basin: constraints on the development of the miocene retroarc foreland basin, south-central andes. *Lithosphere* 10 (3), 366–391. doi:10.1130/l709.1

Carrapa, B., DeCelles, P. G., Ducea, M. N., Jepson, G., Osakwe, A., Balgord, E., et al. (2022). Estimates of paleo-crustal thickness at Cerro Aconcagua (southern central andes) from detrital proxy-records: implications for models of continental arc evolution. *Earth Planet. Sci. Lett.* 585, 117526. doi:10.1016/j.epsl.2022.117526

Cegarra, M. I. (1994). *La faja plegada y corrida de la cordillera principal entre Puente del Inca y Las Cuevas*. Alta Cordillera de Mendoza, Argentina: University of Buenos Aires. PhD thesis.

Cegarra, M. I., and Ramos, V. A. (1996). "La faja plegada y corrida del Aconcagua," in *Geología de la región del Aconcagua, provincias de San Juan y Mendoza*. Editors V. A. Ramos, M. B. Aguirre-Urreta, P. P. Álvarez, M. I. Cegarra, E. O. Cristallini, S. M. Kay, et al. (Buenos Aires: Anales de la Dirección Nacional del Servicio Geológico, Subsecretaría de Minería de la Nación), 387–422.

Charrier, R., Baeza, O., Elgueta, S., Flynn, J. J., Gans, P., Kay, S. M., et al. (2002). Evidence for Cenozoic extensional basin development and tectonic inversión south of the flat-slab segment, southern Central Andes, Chile (33°-36° S.L). *J. S. Am. Earth Sci.* 15, 117–139. doi:10.1016/s0895-9811(02)00009-3

Charrier, R., Ramos, V. A., Tapia, F., and Sagripanti, L. (2015). "Tectono-stratigraphic evolution of the andean orogen between 31 and 37°S (Chile and western Argentina)," in *Geodynamic processes in the Andes of Central Chile and Argentina*. Editors S. A. Sepúlveda, L. B. Giambiagi, S. M. Moreiras, L. Pinto, M. Tunik, G. D. Hoke, et al. (London: Special Publications of the Geological Society), 399, 13–61.

Cristallini, E. O., and Ramos, V. A. (1996). "Los depósitos continentales cretácicos y volcanitas asociadas," in *Geología de la región del Aconcagua, provincias de San Juan y Mendoza*. Editors V. A. Ramos, M. B. Aguirre-Urreta, P. P. Álvarez, M. I. Cegarra, E. O. Cristallini, S. M. Kay, et al. (Buenos Aires: Anales de la Dirección Nacional del Servicio Geológico, Subsecretaría de Minería de la Nación), 231–273.

Darwin, C. (1846). *Geological observations on south America*. London: Smith, Elder and Company.

Deckart, K., Clark, A. H., Celso, A. A., Ricardo, V. R., Bertens, A. N., Mortensen, J. K., et al. (2005). Magmatic and hydrothermal chronology of the gian Río Blanco porphyry copper deposit, Central Chile: implications of and integrated u-pb and ^{40}ar/^{39}ar database. *Econ. Geol.* 100 (5), 905–934. doi:10.2113/gsecongeo.100.5.905

Dickinson, W. R., and Gehrels, G. E. (2009). Use of U-Pb ages of detrital zircons to infer maximum depositional ages of strata: A test against a Colorado plateau mesozoic database. *Earth Planet. Sci. Lett.* 288 (1-2), 115–125. doi:10.1016/j.epsl.2009.09.013

Farías, M., Charrier, R., Carretier, S., Martinod, J., Fock, A., Camplbell, D., et al. (2008). Late Miocene high and rapid surface uplift and its erosional response in the Andes of central Chile (33°-35°S). *Tectonics* 27, TC1005. doi:10.1029/2006TC002046

Farías, M., Comte, D., Charrier, R., Martinod, J., David, C., Tassara, A., et al. (2010). Crustal-scale structural architecture in central Chile based on seismicity and surface geology: implications for andean mountain building. *Tectonics* 29, 2009TC002480. doi:10.1029/2009TC002480

Fennell, L. M., Folguera, A., Naipauer, M., Gianni, G., Rojas Vera, E., Bottesi, G., et al. (2017). Cretaceous deformation of the southern central andes: synorogenic growth strata in the neuquén group (35°30'-37°s). *Basin Res.* 29 (1), 51–72. doi:10.1111/bre.12135

Fock, A., Charrier, R., Farías, M., and Muñoz, M. (2006). Fallas de vergencia oeste en la Cordillera principal de Chile central: inversión de la cuenca de abanico (33°-34°s). *Ser. Publicación Espec. Asoc. Geol. Argent.* 6, 48–55.

Fuentes, F., Vergara, M., Aguirre, L., and Feraud, G. (2002). Contact relationships of tertiary volcanic units from the andes of central Chile (33°S): A reinterpretation based on ^{40}Ar/^{39}Ar dating. *Rev. Geol. Chile* 29, 207–225.

Gana, P., and Wall, R. (1997). Ar-40/Ar-39 and K-Ar geochronological evidences of an Upper Cretaceous Eocene hiatus in central Chile (33-33°30'S). *Rev. Geol. Chile* 24, 145–163.

Gansser, A. (1973). Facts and theories on the andes. *J. Geol. Soc. Lond.* 129, 93–131. doi:10.1144/gsjgs.129.2.0093

Gehrels, G. (2014). Detrital zircon U-Pb geochronology applied to tectonics. *Annu. Rev. Earth Planet. Sci.* 42, 127–149. doi:10.1146/annurev-earth-050212-124012

Giambiagi, L. B., Álvarez, P. P., Godoy, E., and Ramos, V. A. (2003a). The control of pre-existing extensional structures on the evolution of the southern sector of the Aconcagua fold and thrust belt, southern Andes. *Tectonophysics* 369, 1–19. doi:10.1016/S0040-1951(03)00171-9

Giambiagi, L. B., Ramos, V. A., Godoy, E., Álvarez, P. P., and Orts, S. (2003b). Cenozoic deformation and tectonic style of the Andes, between 33° and 34° south latitude. *Tectonics* 22 (4), 1041. doi:10.1029/2001TC001354

Giambiagi, L. B., and Ramos, V. A. (2002). Structural evolution of the Andes in a transitional zone between flat and normal subduction (33°30'-33°45'S), Argentina and Chile. *J. S. Am. Earth Sci.* 15, 101–116. doi:10.1016/S0895-9811(02)00008-1

Giambiagi, L., Mescua, J., Bechis, F., Tassara, A., and Hoke, G. (2012). Thrust belts of the southern central andes: along-strike variations in shortening, topography, crustal geometry, and denudation. *GSA Bull.* 124 (7/8), 1339–1351. doi:10.1130/B30609.1

Giambiagi, L., Mescua, J., Heredia, N., Farías, P., García Sansegundo, J., Fernández, C., et al. (2014). Reactivation of Paleozoic structures during Cenozoic deformation in the Cordón del Plata and Southern Precordillera ranges (Mendoza, Argentina). *J. Iber. Geol.* 40 (2), 309–320. doi:10.5209/rev_JIGE.2014.v40.n2.45302

Giambiagi, L., Quiroga, R., Bechis, F., Barrionuevo, M., and Mescua, J. (2022b). "Natural examples of regional-scale structures from the southern central andes and patagonian andes," in *Andean structural styles: A seismic atlas*. Editors G. Zamora, and A. Mora (Amsterdam, Netherlands: Elsevier), 83–96.

Giambiagi, L., Tassara, A., Echaurren, A., Julve, J., Quiroga, R., Barrionuevo, A., et al. (2022a). Crustal anatomy and evolution of a subduction-related orogenic system: insights from the southern central andes (22-35°s). *Earth-Science Rev.* 232, 104138. doi:10.1016/j.earscirev.2022.104138

Giambiagi, L., Tassara, A., Mescua, J., Tunik, M., Álvarez, P. P., Godoy, E., et al. (2015). "Evolution of shallow and deep structures along the maipo-tunuyán transect (33°40'S): from the pacific coast to the andean foreland," in *Geodynamic processes in the Andes of Central Chile and Argentina*. Editors S. A. Sepúlveda, L. B. Giambiagi, S. M. Moreiras, L. Pinto, M. Tunik, G. D. Hoke, et al. (London: Special Publications of the Geological Society), 399, 63–82.

Gómez, R., Lothari, L., Tunik, M., and Casadio, S. (2019). Onset of foreland basin deposition in the neuquén basin (34°-35°S): new data from sedimentary petrology and u-pb dating of detrital zircons from the upper cretaceous non-marine deposits. *J. S. Am. Earth Sci.* 95, 102257. doi:10.1016/j.jsames.2019.102257

Gonzáles Bonorino, F. (1950). Geologic cross-section of the Cordillera de los Andes at about parallel 33° L.S. (Argentina-Chile). *Bull. Geol. Soc. Am.* 61, 17–26. doi:10.1130/0016-7606(1950)61[17:gcotcd]2.0.co;2

Groeber, P. (1951). La alta cordillera entre las latitudes 34° y 29°30'. *Rev. del Inst. Nac. Investig. las Ciencias Nat.* 1, 235–352.

Hoke, G. D., Graber, N. R., Mescua, J. F., Giambiagi, L. B., Fitzgerald, P. G., and Metcalf, J. R. (2015). "Near pure surface uplift of the Argentine frontal cordillera: insights from (u-th)/he thermochronometry and geomorphic analysis," in *Geodynamic processes in the Andes of Central Chile and Argentina*. Editors S. A. Sepúlveda, L. B. Giambiagi, S. M. Moreiras, L. Pinto, M. Tunik, G. D. Hoke, et al. (London: Special Publications of the Geological Society), 399, 383–399.

Horton, B. K., and Folguera, A. (2022). "Tectonic inheritance and structural styles in the Andean fold-thrust belt and foreland basin," in *Andean structural styles: A seismic atlas*. Editors G. Zamora, and A. Mora (Amsterdam, Netherlands: Elsevier), 83–96.

Horton, B. K., Fuentes, F., Boll, A., Starck, D., Ramirez, S. G., and Stockli, D. F. (2016). Andean stratigraphic record of the transition from backarc extension to orogenic shortening: A case study from the northern neuquén basin, Argentina. *J. S. Am. Earth Sci.* 71, 17–40. doi:10.1016/j.jsames.2016.06.003

Inca Garcilazo de la Vega, I. (1609). *Comentarios reales de los Incas*. Lima: Editorial Universo S.A. 1963.

Kley, J., Monaldi, C. R., and Salfity, J. A. (1999). Along-strike segmentation of the andean foreland: causes and consequences. *Tectonophysics* 301, 75–94. doi:10.1016/s0040-1951(98)90223-2

Lo Forte, G. (1996). "Los depósitos jurásicos de la Alta cordillera de Mendoza," in *Geología de la región del Aconcagua, provincias de San Juan y Mendoza*. Editors V. A. Ramos, M. B. Aguirre-Urreta, P. P. Álvarez, M. I. Cegarra, E. O. Cristallini, S. M. Kay, et al. (Buenos Aires: Anales de la Dirección Nacional del Servicio Geológico, Subsecretaría de Minería de la Nación), 139–178.

Lossada, A. C., Hoke, G. D., Giambiagi, L. B., Fitzgerald, P. G., Mescua, J. F., Suriano, J., et al. (2020a). Detrital thermochronology reveals major middle miocene exhumation of the eastern flank ofthe andes that predates the PampeanFlat slab (33°–33.5°S). *Tectonics* 39, e2019TC005764. doi:10.1029/2019TC005764

Lossada, A. C., Suriano, J., Giambiagi, L., Fitzgerald, P. G., Hoke, G., Mescua, J., et al. (2020b). Cenozoic exhumation history at the core of the Andes at 31.5°S revealed by apatite fission track thermochronology. *J. S. Am. Earth Sci.* 103, 102751. doi:10.1016/j.jsames.2020.102751

Ludwig, K. R. (1999). User's manual for isoplot/ex, version 2.10, A geochronological toolkit for Microsoft Excel. *Special Publ. Berkeley Geochronological Cent.* 1, 46.

Mackaman-Lofland, C., Horton, B. K., Fuentes, F., Constenius, K. N., and Stockli, D. F. (2019). Mesozoic to cenozoic retroarc basin evolution during changes in tectonic regime, southern central andes (31-33°S): insights from zircon u-pb geochronology. *J. S. Am. Earth Sci.* 89, 299–318. doi:10.1016/j.jsames.2018.10.004

Mardones, V., Peña, M., Pairoa, S., Ammirati, J. B., and Leisen, M. (2021). Architecture, kinematics, and tectonic evolution of the principal cordillera of the andes in central Chile (~33.5°S): insights from detrital zircon u-pb geochronology and seismotectonics implications. *Tectonics* 40, e2020TC006499. doi:10.1029/2020TC006499

Martos, F. E., Fennell, L. M., Brisson, S., Palmieri, G., Naipauer, M., and Folguera, A. (2020). Tectonic evolution of the northern Malargüe fold and thrust belt, Mendoza province, Argentina. *J. S. Am. Earth Sci.* 103, 102711. doi:10.1016/j.jsames.2020.102711

Martos, F. E., Naipauer, M., Fennell, L. M., Acevedo, E., Hauser, N., and Folguera, A. (2022). Neogene evolution of the Aconcagua fold-and-thrust belt: linking structural, sedimentary analyses and provenance u-pb detrital zircón data for the penitentes basin. *Tectonophysics* 825, 229233. doi:10.1016/j.tecto.2022.229233

Mescua, J. F., Giambiagi, L. B., and Bechis, F. (2008). Evidencias de tectónica extensional en el Jurásico Tardío (Kimmeridgiano) del suroeste de la provincia de Mendoza. *Rev. Asoc. Geol. Argent.* 63 (4), 512–519.

Montecinos, P., Schärer, U., Vergara, M., and Aguirre, L. (2008). Lithospheric origin of oligocene-miocene magmatism in Central Chile: U-Pb ages and Sr-Pb-Hf isotope composition of minerals. *J. Petrology* 49 (3), 555–580. doi:10.1093/petrology/egn004

Morel, L., Fennell, L. M., Naipauer, M., Folguera, A., and Pérez-Frasette, M. (2023). Characterization and stratigraphic review of the upper jurassic-lower cretaceous Mendoza Group in the Blanco river valley (~33°SL). *J. S. Am. Earth Sci.* 124, 104252. doi:10.1016/j.jsames.2023.104252

Mouthereau, F., Watts, A. B., and Burov, E. (2013). Structure of orogenic belts controlled by lithosphere age. *Nat. Geosci.* 6, 785–789. doi:10.1038/ngeo1902

Munizaga, F., and Vicente, J. C. (1982). Acerca de la zonación plutónica y del volcanismo miocenico en los andes de Aconcagua (lat. 32-33°S): datos radiométricos k-ar. *Rev. Geol. Chile* 16, 3–21.

Nyström, J. O., Vergara, M., Morata, D., and Levi, B. (2003). Tertiary volcanism during extension in the Andean foothills of central Chile (33°15'-33°45'S). *GSA Bull.* 115 (12), 1523–1537. doi:10.1130/B25099.1

Olivar, J., Nacif, S., Fennell, L., and Folguera, A. (2018). Within plate seismicity analysis in the segment between the high Cordillera and the Precordillera of northern Mendoza (Southern Central Andes). *Geodesy Geodyn.* 9, 13–24. doi:10.1016/j.geog.2017.09.004

Orts, S., and Ramos, V. A. (2006). Evidence of middle to late cretaceous compressive deformation in the high andes of Mendoza, Argentina. *Abstr. Backbone Am. Meet.* 5, 65.

Parras, A. M., Casadío, S., and Pires, M. (1998). Secuencias depositacionales del Grupo Malargüe y el Límite Cretácico-Paleógeno, en el sur de la provincia de Mendoza, Argentina. *Publicación Espec. Asoc. Paleontológica Argent.* 5, 61–69.

Pérez, D. J., and Ramos, V. A. (1996). "El basamento prejurásico," in *Geología de la región del Aconcagua, provincias de San Juan y Mendoza*. Editors V. A. Ramos, M. B. Aguirre-Urreta, P. P. Álvarez, M. I. Cegarra, E. O. Cristallini, S. M. Kay, et al. (Buenos Aires: Anales de la Dirección Nacional del Servicio Geológico, Subsecretaría de Minería de la Nación), 27–58.

Piquer, J., Skarmeta, J., and Cooke, D. R. (2015). Structural evolution of the Río blanco-los bronces district, andes of Central Chile: controls on stratigraphy, magmatism, and mineralization. *Econ. Geol.* 110, 1995–2023. doi:10.2113/econgeo.110.8.1995

Ramos, V. A., Aguirre-Urreta, M. B., Álvarez, P. P., Colluccia, A., Giambiagi, L., Pérez, D. J., et al. (2010). *Hoja geológica 3369-III Cerro Tupungato, escala 1:250.000*. Buenos Aires: Boletín N° 386 del Servicio Geológico Minero Argentino.

Ramos, V. A. (2009). "Anatomy and global context of the andes: main geologic features and the andean orogenic cycle," in *Backbone of the Americas: Ridge collision, shallow subduction and plateau uplift*. Editors S. M. Kay, V. A. Ramos, and W. R. Dickinson (United states: Memoir 204 of the Geological Society of America), 31–65. doi:10.1130/2009.1204(02

Ramos, V. A., Cegarra, M. Y., and Pérez, D. J. (1996a). "Carta geológica Región del Aconcagua, escala 1:100.000," in *Geología de la región del Aconcagua, provincias de San Juan y Mendoza*. Editors V. A. Ramos, M. B. Aguirre-Urreta, P. P. Álvarez, M. I. Cegarra, E. O. Cristallini, S. M. Kay, et al. (Buenos Aires: Anales de la Dirección Nacional del Servicio Geológico, Subsecretaría de Minería de la Nación).

Ramos, V. A., Cristallini, E. O., and Pérez, D. J. (2002). The pampean flat-slab of the central andes. *J. S. Am. Earth Sci.* 15, 59–78. doi:10.1016/s0895-9811(02)00006-8

Ramos, V. A. (1985b). El mesozoico de la alta cordillera de Mendoza: facies y desarrollo estratigráfico – argentina. *Actas del IV° Congr. Geol. Chil.* 1 (1), 492–513.

Ramos, V. A. (1985a). El mesozoico de la alta cordillera de Mendoza: reconstrucción tectónica de sus facies – argentina. *Actas del IV° Congr. Geol. Chil.* 1 (2), 104–118.

Ramos, V. A., Kay, S. M., and Pérez, D. J. (1996b). "El volcanismo de la región del Aconcagua," in *Geología de la región del Aconcagua, provincias de San Juan y Mendoza*. Editors V. A. Ramos, M. B. Aguirre-Urreta, P. P. Álvarez, M. I. Cegarra, E. O. Cristallini, S. M. Kay, et al. (Buenos Aires: Anales de la Dirección Nacional del Servicio Geológico, Subsecretaría de Minería de la Nación), 297–316.

Ramos, V. A. (1999). Plate tectonic setting of the andean cordillera. *Episodes* 22 (3), 183–190. doi:10.18814/epiiugs/1999/v22i3/005

Ramos, V. A. (1988). The tectonics of the Central Andes; 30° to 33° S latitude. *Special Pap. Geol. Soc. Am.* 218, 31–54. doi:10.1130/SPE218-p31

Riesner, M., Lacassin, R., Simoes, M., Armijo, R., Rauld, R., and Vargas, G. (2017). Kinematics of the active West Andean fold-and-thrust belt (central Chile): structure and long-term shortening rate. *Tectonics* 36, 287–303. doi:10.1002/2016TC004269

Riesner, M., Lacassin, R., Simoes, M., Carrizo, D., and Armijo, R. (2018). Revisiting the crustal structure and kinematics of the central andes at 33.5°S: implications for the mechanics of andean mountain building. *Tectonics* 37, 1347–1375. doi:10.1002/2017TC004513

Riesner, M., Simoes, M., Carrizo, D., and Lacassin, R. (2019). Early exhumation of the frontal cordillera (southern central andes) and implications for Andean mountainmountain-building at ~33.5°S. *Sci. Rep.* 9, 7972. doi:10.1038/s41598-019-44320-1

Rivano, S., Sepúlveda, P., Boric, R., and Espiñeira, D. (1993). *Hojas quillota y portillo, escala 1:250.000*. Santiago: Carta Geológica de Chile N° 73 del Servicio Nacional de Geología y Minería.

Sanguinetti, A. S., and Cegarra, M. I. (1991). El volcanismo jurasico superior al este de las Cuevas, Cordillera Principal de Mendoza, Argentina. *Resúmenes Expand. del VI Congr. Geol. Chil.*, 872–876.

Sanguinetti, A. S. (1989). Volcanismo neojurasico-neocomiano de la quebrada de Vargas, Alta Cordillera de Mendoza. *Rev. Asoc. Geol. Argent.* XLIV (1-4), 381–393.

Scazziota, M., Fernández Paz, L., Iannelli, S., Fennell, L., Folguera, A., and Litvak, V. (2022). "Edad, litofacies y caracterización estructural del volcanismo mioceno en la Cordillera Principal de Mendoza (33°S)," in Actas del XXI Congreso Geológico Argentino, Chubut, Argentina, 14 March 2022 - 18 March 2022.

Schiller, W. (1912). La Alta Cordillera de San Juan y Mendoza y parte de la provincial de San Juan. *An. del Minist. Agric. Minería* 7 (5), 1–68.

Taucare, M., Roquer, T., Heuser, G., Pérez-Estay, N., Arancibia, G., Yáñez, G., et al. (2022). Selective reactivation of inherited fault zones driven by stress field changes: insights from structural and paleostress analysis of the pocuro fault zone, southern central andes (32.8°s). *J. S. Am. Earth Sci.* 118, 103914. doi:10.1016/j.jsames.2022.103914

Tunik, M. (2003). Interpretación paleoambiental de los depósitos de la Formación Saldeño (Cretácico superior), en la alta Cordillera de Mendoza, Argentina. *Rev. Asoc. Geol. Argent.* 58 (3), 417–433.

Vennari, V. (2016). Tithonian ammonoids (cephalopoda, ammonoidea) from the Vaca Muerta Formation, neuquén basin, west-central Argentina. *Paleontogr. Abt. A Paleozoology – Stratigr.* 306 (1-6), 85–165. doi:10.1127/pala/306/2016/85

Vermeesch, R. (2018). IsoplotR: A free and open toolbox for geochronology. *Geosci. Front.* 9, 1479–1493. doi:10.1016/J.GSF.2018.04.001

Vicente, J. C. (1972). Aperçu sur l'organisation et l'évolution des Andes argentino-chiliennes centrales au parallèle de l'Aconcagua. *Abstr. XXIV Int. Geol. Congr.* 3, 424–436.

Vicente, J. C., Charrier, R., Davidson, J., Mpodozis, C., and Rivano, S. (1973). La orogenesis subhercinica: fase mayor de la evolución paleogeográfica y estructural de los andes argentino-chilenos centrales. *Actas del V° Congr. Geol. Argent.* 5, 81–98.

Vicente, J. C. (2005). La fase primordial de estructuración de la faja plegada y corrida del Aconcagua: importancia de la fase pehuenche del mioceno inferior. *Rev. Asoc. Geol. Argent.* 60 (4), 672–684.

Vicente, J. C., and Leanza, H. A. (2009). El frente de corrimiento andino al nivel de los cerros penitentes y Visera (alta cordillera de Mendoza): aspectos cronológicos y cartográficos. *Rev. Asoc. Geol. Argent.* 65 (1), 97–110.

Von Gosen, W. (1992). Structural evolution of the Argentine precordillera: the río san juan section. *J. Struct. Geol.* 14 (6), 643–667. doi:10.1016/0191-8141(92)90124-f

Yrigoyen, M. R. (1972). "Cordillera principal," in *Geología regional Argentina*. Editor A. F. Leanza (Córdoba: Academia Nacional de Ciencias), 345–364.

Yrigoyen, M. R. (1979). "Cordillera principal," in *Geología regional Argentina*. Editor J. C. M. Turner (Córdoba: Academia Nacional de Ciencias), 651–694.

Yrigoyen, M. R. (1976). Observaciones geológicas alrededor del Aconcagua. *Actas del I° Congr. Geol. Chil.* 1, 168–190.